

UNNATURAL LIGANDS FOR ENGINEERED PROTEINS: New Tools for Chemical Genetics

Anthony Bishop, Oleksandr Buzko*, Stephanie Heyeck-Dumas, Ilyoung Jung*, Brian Kraybill*, Yi Liu, Kavita Shah, Scott Ulrich*, Laurie Witucki, Feng Yang, Chao Zhang*, and Kevan M. Shokat*†

Department of Chemistry, Princeton University, Princeton, New Jersey 08544;
e-mail: shokat@cmp.ucsf.edu

Key Words protein engineering, orthogonal ligands, signal transduction, protein design

Abstract Small molecules that modulate the activity of biological signalling molecules can be powerful probes of signal transduction pathways. Highly specific molecules with high affinity are difficult to identify because of the conserved nature of many protein active sites. A newly developed approach to discovery of such small molecules that relies on protein engineering and chemical synthesis has yielded powerful tools for the study of a wide variety of proteins involved in signal transduction (G-proteins, protein kinases, 7-transmembrane receptors, nuclear hormone receptors, and others). Such chemical genetic tools combine the advantages of traditional genetics and the unparalleled temporal control over protein function afforded by small molecule inhibitors/activators that act at diffusion controlled rates with targets.

CONTENTS

INTRODUCTION	578
ENGINEERING UNNATURAL CELL-SIGNALING PATHWAYS	
WITH CHEMICAL GENETICS	579
Switching a GTPase into an XTPase	579
The Specificity Switch from GTP to XTP Is Generalizable	581
Seven-Transmembrane Receptors Activated Solely by Synthetic Ligands	584
Protein Kinases with Specificity for Unnatural Nucleotides	588
Uniquely Inhibitable Protein Kinases	590
Conditional Alleles of Kinesin and Myosin Motors	593

*Current address: Department of Cellular and Molecular Pharmacology, University of California, San Francisco, CA.

†Current address: Department of Chemistry, University of California, Berkeley, Berkeley, CA.

Conditional Alleles of Nuclear Hormone Receptors	596
ENGINEERING SIGNALING PATHWAYS FOR HUMAN THERAPY	598
Antibody-Directed Enzyme Prodrug Therapy	598
Initiation of Signals with Chemical Inducers of Dimerization	600
CONCLUSIONS AND FUTURE DIRECTIONS	604

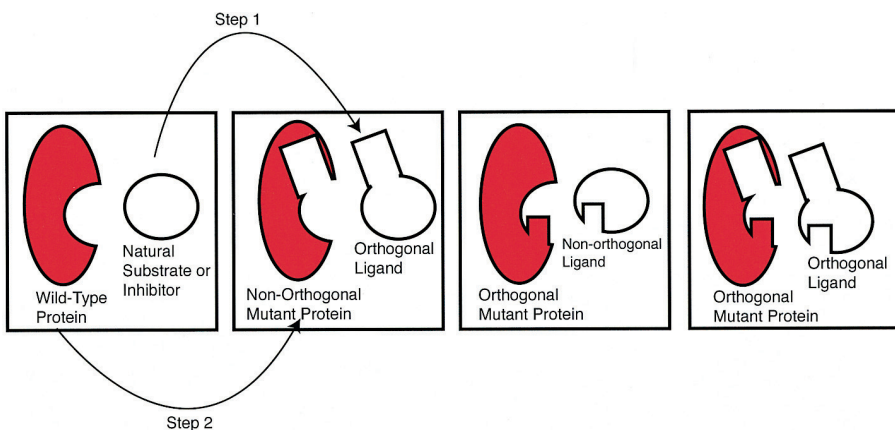
INTRODUCTION

The power of genetic approaches to the study of protein function is the ability to affect the activity of a single protein in a whole organism; yet the use of genetics to alter protein function is not an ideal process, because protein levels respond very slowly to changes at the gene level. In contrast, the use of small synthetic molecules or natural products to alter protein activity elicit extremely rapid results, because these agents act at diffusion-controlled rates with their targets and do not require operation of cellular transcriptional machinery. The small-molecule approach, however, suffers from problems of specificity, because enzyme inhibitors are often not specific for just one protein in the organism of interest. Furthermore, it is often difficult to determine the true spectrum of action of such small molecules. As tools for studying protein functions, small molecules require extensive characterization before their effects on a complex biological system can be interpreted.

On one hand, genetics offers unprecedented target specificity. On the other hand, the chemical approach offers unprecedented temporal control over the function of target proteins. Experimental systems that incorporate the advantages of both of these approaches are powerful tools for studying protein function in the postgenomic era.

Recently, the benefits of combining these two approaches have been demonstrated through a number of studies in diverse areas of cell biology and chemistry. All of these studies have used the same fundamental approach. First, a small molecule that binds to the protein of interest is modified in a manner that eliminates its ability to bind to its target. This modified ligand is said to be “orthogonal” in normal cells because it is completely silent (noninteracting with the natural system), in contrast to its unmodified counterpart (Scheme A). Second, the individual protein of interest is engineered to accept the orthogonal ligand (substrate, inhibitor, activator, etc). It is important that the mutation to the protein must affect only binding to the orthogonal ligand and not introduce any other modification to protein function. In some situations the engineered protein may not accept the natural ligand, thus creating a protein that itself is orthogonal. (In this situation, the protein functions as a conditional allele).

This simultaneous engineering of the target of interest and derivatization of the small molecule are similar in genetic terms to a suppressor screen, which can reveal obligate interactions between two proteins. The unprecedented specificity of such systems arises because the degeneracy of the natural system (multiple proteins that use the same substrate) is broken down to create the ideal “one-ligand/one-protein” system.



Scheme A Operational definition of orthogonal ligands and orthogonal proteins.

This review focuses on the use of small molecules to elucidate gene function, using engineered proteins and unnatural ligands. Several excellent recent reviews have described analogous approaches to engineering protein-protein interactions (1–3).

ENGINEERING UNNATURAL CELL-SIGNALING PATHWAYS WITH CHEMICAL GENETICS

Switching a GTPase into an XTPase

The first engineered protein in a signal transduction pathway to accept an unnatural substrate was a member of the GTPase family of enzymes (4). GTPases control many biological processes, including translation, protein translocation, vesicle transport, nuclear import, and signal transduction. GTPases typically exist in both GTP- and GDP-bound states. The enzymes interchange between these two states by hydrolyzing bound GTP to GDP + P_i, followed by binding of GTP. Several different effector proteins can accelerate the interchange between the two states either by acceleration of GTP hydrolysis (GTPase-activating proteins) or by the exchange of GTP for GDP (guanine nucleotide exchange factors).

One of the best characterized roles of GTPases is in protein biosynthesis. EF-Tu is a GTPase that is responsible for loading amino-acyl transfer RNAs onto the ribosome during protein biosynthesis. EF-Tu not only loads the amino-acyl transfer RNA but is also responsible for hydrolyzing the amino acid from the transfer RNA if it is not the amino acid coded for by the messenger RNA.

What is the energy cost (i.e. number of GTPs hydrolyzed per amino acid loading step) involved in this process? The problem with making this measurement is that another GTPase (EF-G) is intimately coupled to EF-Tu's function during ribosomal protein synthesis. EF-G is responsible for translocation of the ribosome after each successive peptide bond formation step. Hwang & Miller (4) proposed that the role of EF-Tu could be distinguished from that of EF-G by engineering EF-Tu to accept a nucleotide other than GTP.

Analysis of the highly conserved GTP-binding motif revealed several hydrogen bonds between amino-acid side chains in EF-Tu and the guanine base of GTP (Figure 1A, see color insert). Hwang & Miller (4) used site-directed mutagenesis to disrupt one key H bond, between Asp-138 and the C² exocyclic amine of GTP. Mutation of Asp-138 → Asn disrupted the H-bond acceptor function of Asp-138, and replaced it with an H-bond donor. The presence of an H-bond donor opposite the exocyclic amine of GTP produces a repulsive (donor-donor) interaction that Hwang & Miller (4) accurately predicted would lead to the inability of Asp-138–Asn–EF-Tu to accept GTP as a substrate.

A surrogate for GTP was chosen that contains an H-bond acceptor at the C2 position, XTP (Figure 1B). The xanthine base perfectly complements the mutation in EF-Tu by providing an H-bond acceptor functionality (carbonyl) to the new H-bond donor residue (Asn-135). The mutation of Asp-138 → Asn produces an XTP-dependent allele of EF-Tu. This elegantly designed mutation and chemical

TABLE 1 Consensus sequences in the GTPase super family

	Phosphate and Mg ²⁺ binding			Guanine ring binding	
	G1	G2	G3	G4	G5
Consensus sequence	GXXXXGK (S/T)	D(X) _n T	DXXG	NKXD	TXAX
H/K/N-Ras human	GAGGVGKS ₁₇	DEYDPTI ₃₆	DTAG ₆₀	NKCD ₁₁₉	TSAK ₁₄₇
G proteins mammalian	GAGESGKS	D(X) ₇ TT	DVGG	NKKD	TCAT
Transposase P element	GLKKSWKO ₂₆₈	DPDTL ₂₈₃	DVDSG ₃₅₅	NKSD ₃₉₆	TTAS ₄₁₄

complementation work surprisingly well, in that the kinetic constants of the mutant with the designed substrate (XTP) are indistinguishable from those of the wild-type enzyme with the natural substrate, GTP (5). Hwang & Miller (4) suggested that, because the motif NKXD (G4 consensus region) is conserved in all known GTPases, the mutation of Asp → Asn should convert any GTPase into an XTPase (Table 1). This in fact has been the case, as evidenced by the use of this particular strategy to elegantly decouple single GTPases in many complex pathways (Table 2).

With the (D138N) EF-Tu XTPase in hand, Weijland & Parmengiani (5) determined the energy cost of nucleotide hydrolysis by EF-Tu. Poly(U)-directed poly (phenylalanine) synthesis was carried out in an *in vitro* translation experiment in the presence of the XTPase (D138N-EF-Tu), the GTPase-EF-G, ribosomes, and all necessary components of ribosomal protein biosynthesis, including GTP and [γ -³²P]XTP (Figure 2, see color insert). By careful quantitation of the $^{32}\text{PO}_4^{2-}$ produced during each amino acid-coupling cycle, these authors were able to determine that two cycles of EF-Tu-mediated nucleotide hydrolysis occurred during each amino acid coupling. Previously it had been impossible to determine

TABLE 2 GTPases that have been successfully engineered to accept XTP

GTPase	XTPase	Function	References
EF-Tu	D138N	Protein biosynthesis	4, 5
Adenylosuccinate	D333N	Purine nucleotide metabolism	74
FtsY	D441N	Signal recognition particle receptor	6
Ypt1	D124N	Regulation of endoplasmic reticulum to Golgi vesicle trafficking	7, 15
HypB	D241N	Nickel insertion into hydrogenases	75
Ran	D125N	Nuclear protein import	9
p21Ras	D119N	Control of MAPK pathway	13
Rab5	D136N	Endo- and exocytic pathways	76
G α _o	D273N/Q205	G protein-coupled receptor pathway	15
P element transposase	D379N	DNA transposition	16

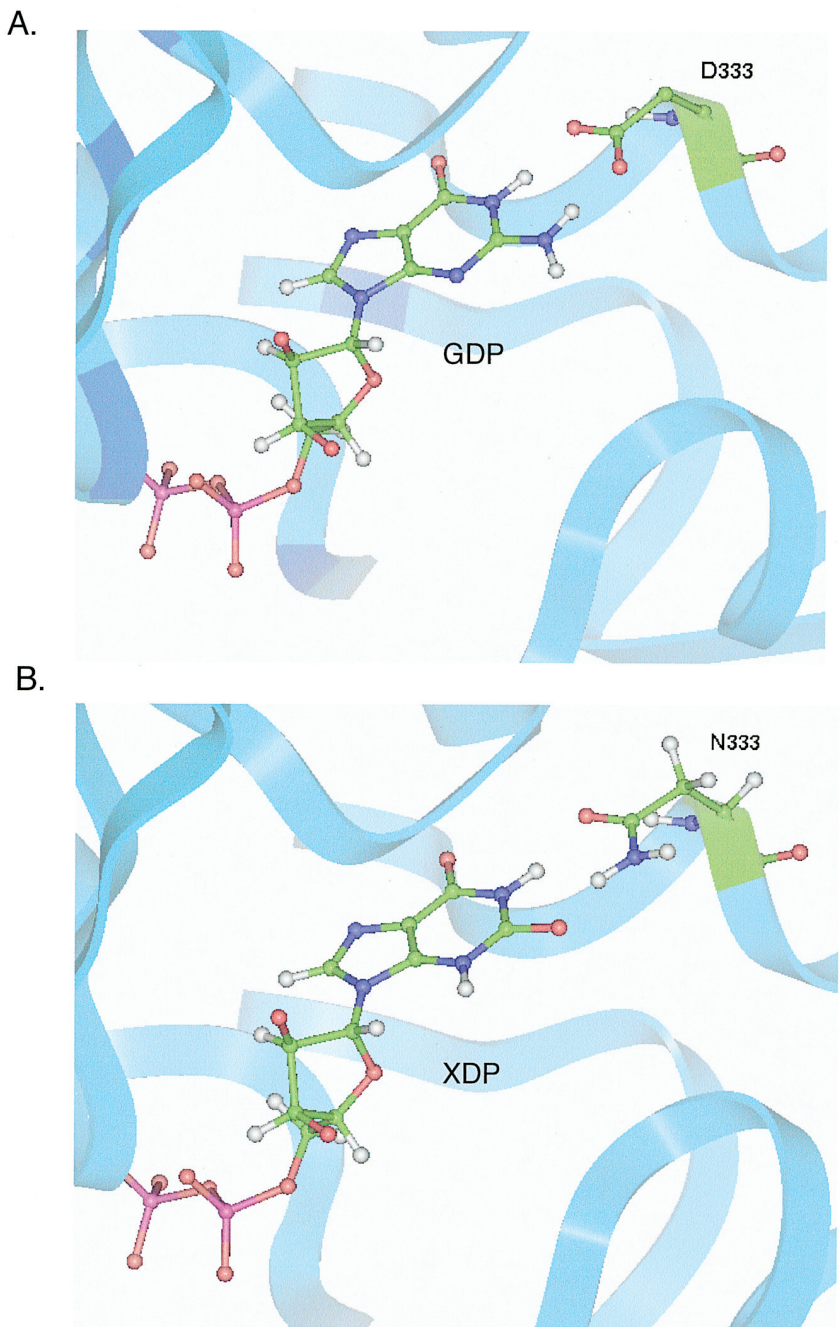


Figure 1 Caption appears at right, on following page.

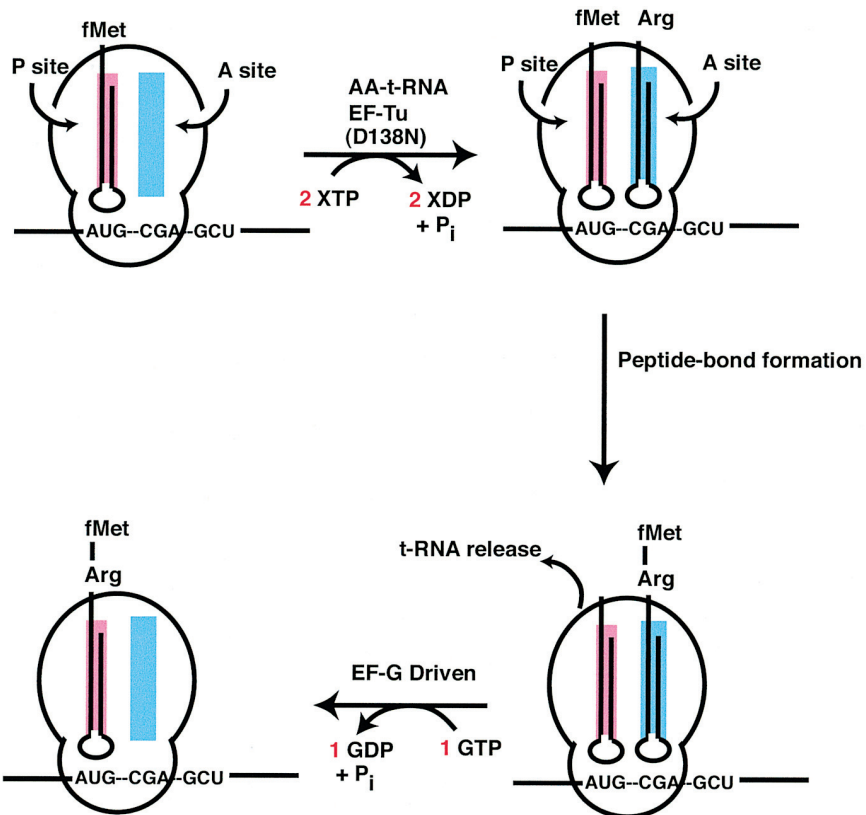


Figure 2 Use of XTP dependent D138N EF-Tu to measure number of XTP ses per amino acid coupling step in ribosomal protein syntheses. Figure derix data in reference 5.

Figure 1 (from page 2) A. Ribbon diagram of GDP bound to Elongation (EF-Tu). GDP is shown in half-and-stick representation, with a bifurcated b aspartate 138 (D138) also shown in half-and-stick representation. Atom c green = carbon, red = oxygen, blue = nitrogen, white = hydrogen, purple = phosph. Hypothetical structure the orthogonal ligand, xanthine diphosphat (XPD), the orthogonal EF-Tu mutant (D138N EF-Tu).

whether the amino-acyl-loading step (EF-Tu) or the translocation step (EF-G) was more energy demanding. This finding suggests that, in an as-yet-undefined way, two different GTP-loaded EF-Tu molecules interact with the ribosome during each amino acid-loading cycle.

The Specificity Switch from GTP to XTP Is Generalizable

Mutation of the conserved aspartate to asparagine in the highly conserved GTP-binding consensus motif (NKXD) has been exploited to probe the function of individual GTPases in complex cell lysates as well as in whole cells (Table 2).

Powers & Walter investigated the *Escherichia coli* GTPases Ffh and FtsY, which are homologs of essential components of the eukaryotic signal recognition particle and its receptor, respectively (6). Ffh and FtsY are GTPases that catalyze the cotranslational targeting of proteins to the bacterial plasma membrane. To understand the role of each GTP-binding site and GTP/GDP-binding cycle, the FtsY (D441N) mutant was created, which accepted only XTP as a substrate and did not accept GTP. After measurement of the GTPase and XTPase activities of Ffh, and FtsY (D441N), respectively, at different nucleotide concentrations, Powers & Walter (6) showed that Ffh stimulated XTP hydrolysis by FtsY (D441N) in the presence of 4.5S RNA and that FtsY (D441N) similarly stimulated GTP hydrolysis by Ffh in a reaction that required XTP. Thus, nucleotide hydrolysis by Ffh and FtsY appears to occur by a reciprocally coupled reaction in which each GTPase acts as a GTPase-activating protein for the other GTPase; therefore, Powers & Walters (6) used the XTPase mutation in this system to uncover a novel way in which GTPases themselves can regulate the GTPase activity of their associated proteins.

The XTPase mutation has been used to create selectively inhibitable mutants of the GTPase of interest. Jones et al (7) engineered the yeast Rab family member Ypt1 to accept XTP rather than GTP, by mutation of aspartate-124 to asparagine, producing the Ypt1 mutant D124N, which was expressed in yeast and acted in a dominant fashion to confer growth inhibition and block protein secretion. Because D124N does not bind GTP or GDP, the dominant inhibitory function of this mutant can be ascribed to the nucleotide-free form of the enzyme. Because function of the Ypt1 mutant (D124N) is dominant negative only in the absence of a competent nucleotide, the inhibition can be relieved by the addition of XTP in an *in vitro*-reconstituted system. Jones et al (7) proposed that the nucleotide-free form of Ypt1 (D124N) acted dominantly by sequestering the GTP exchange factor from wild-type Ypt1, thus inhibiting the vesicular transport pathway.

Another elegant use of the XTPase mutation has been in combination with nonhydrolyzable GTP analogs. Because the only active site inhibitors of GTPases are nonhydrolyzable analogs of GTP, such as GTP(γ S), such reagents inhibit all GTPases in a cell or cell lysate. The lack of selective inhibitors has made answering even the simple question of whether one or more GTPases are required for a given cell-signaling pathway very difficult. Signal-dependent transport of proteins into the nucleus was known to involve at least one cytosolic GTPase protein, Ran (8). To investigate whether other GTPases were also involved, the XTPase mutation in

Ran (D125N) was made by two laboratories (9, 10). As expected, the Ran (D125N) mutation was not inhibitable by GTP γ S, thus providing a tool for carrying out an elegant screen for GTPases other than Ran that are important for nuclear import of proteins. Indeed, in an *in vitro* assay, nuclear import can be reconstituted by Ran (D125N)-XTP, yet this pathway remains sensitive to GTP γ S, implicating another unidentified GTPase for the first time. Sweet & Gerace (9) suggest that the unidentified GTPase could be a component of the nuclear pore complex. In principle, candidate GTPases could be turned into XTPases by similar mutagenesis, and their involvement in the nuclear transport pathway could be tested.

The best characterized GTPase, p21Ras, has also been studied by using the XTPase mutational approach (11). It is interesting that, unlike the previous examples of GTPases engineered to accept XTP, the corresponding D119N mutation in p21Ras was originally identified by a random screen for mutants with poor GTP-binding activity (12). These authors characterized the D119N p21Ras mutant in terms of its inability to bind GTP but did not use XTP as a surrogate nucleotide for this mutant. The XTPase activity of p21Ras (D119N) has been characterized in great detail by Schmidt et al (13), especially for the effects of Ras regulators such as GTPase-activating proteins, the guanine nucleotide exchange factor Cdc25^{Mm}, and others. The kinetic constants k_{on} and k_{off} for GDP and XDP for both wild type and the D119N mutant of p21Ras were determined in a fluorescence assay with methylanthraniloyl-substituted nucleotides (Table 3).

The D119N p21Ras exhibits a 10³-fold loss in binding affinity for GDP in comparison with wild-type p21Ras. The kinetic constants reveal that the k_{on} for GDP binding to both proteins is almost unchanged, yet the k_{off} has increased by ~10³ for D119N p21Ras. This rapid dissociation rate for GDP from D119N closely mirrors the fast dissociation of XDP from the wild-type protein, 1150 × 10⁵/s vs 440 × 10⁵/s, respectively (13). This again demonstrates the extremely well-behaved nature of the D-to-N mutation in GTPases and their faithful recapitulation of function, which is dependent on XTP rather than GTP. The remaining kinetic comparisons between the wild type and the D119N mutant of Ras are also quite well matched (Table 3).

Schmidt et al (13) were particularly interested in using the XTP-engineered p21Ras protein to probe Ras signaling in whole cells by altering the cellular pool of XTP-XDP. Previously it was shown that D119N p21Ras is an oncogene even though it does not appreciably bind GTP. As a test of whether XTP concentrations in cells could be increased, Wittinghofer and colleagues (14) measured the inhibition of transforming activity of D119N Ras after microinjection of millimolar concentrations of XTP and XDP, as well as exogenously provided xanthine. Over the 6-h time course of the experiment, no inhibition of the transformed phenotype was observed. This suggests that the intracellular pools of XTP or XDP are not manipulatable, owing to the presence of numerous metabolic enzymes, which interconvert XTP- and GTP-based nucleotides. By a clever strategy, the authors coinjected a preloaded D119N p21Ras protein with XDP and, using a rapid assay for induction of DNA synthesis, showed that the XDP-loaded protein in cells was

TABLE 3 Nucleotide binding of wild-type p21 and p21(D119N) with guanosine and xanthosine nucleotides

Nucleotide	k_{on} (10^6 M s^{-1})	k_{off} (10^{-5} s^{-1})	$K_A = k_{\text{on}}/k_{\text{off}}$ (10^{10} M^{-1})
p21 wild type			
mGDP	1.5	2.0	7.5
mG _{pp} N _p	1.8	36	0.5
mXDP	1.2	440	0.027
mX _{pp} N _p	0.4	(1200)	0.003
GTP _γ S	3.3	9.4	3.5
p21(D119N)			
mGDP	(0.45)	1150	(0.0039)
mXDP	0.51	6.5	0.78
nX _{pp} N _p	1.0	18	0.55

nontransforming for a period of time. After the D119N Ras mutant releases XDP, it regains its transforming activity. Thus, the mutant protein behaves like the wild-type Ras initially after injection and later as an oncogenic protein. These same authors have also recently characterized further mutations to the D119N p21Ras to produce severely dominant negative alleles of this protein (14).

One class of GTPases required additional mutagenesis to the well-described D-to-N mutation. The heterotrimeric G proteins are composed of α , β , and γ subunits. On ligand activation of the seven transmembrane classes of receptor proteins, G α components are induced to exchange GTP for GDP. When G α_0 was engineered by Yu and colleagues (15) to accept XTP by mutation of D273N, the protein lost all ability to bind nucleotides. In a search for second site revertants, these authors used the previously described mutation of Q205L in conjunction with the D273N mutation. Although the glutamine residue at position 205 is at the opposite end of the nucleotide-binding site from aspartate-273, the double mutant was able to accept XTP in the expected fashion. The authors went on to reconstitute G protein-coupled signaling in G α_0 (D273N/Q205L)-transfected COS cells after cell wall permeabilization and the addition of XDP. Thus, the large family of G α GTPases can also be engineered to accept XTP, albeit in the context of an additional mutation in the active site. The structural basis for the ability of the Q205L mutation to rescue XTP binding in the context of the D273N mutation is not known.

In the preceding discussion of the use of GTPase-to-XTPase engineering, the GTPase in question adhered to the well-described consensus sequence shown in Table 1. For the *Drosophila*-encoded P element transposase protein, it was known that GTP was essential for optimal *in vitro* transposition reactions. However, the classic GTP-binding cassette (Table 1) was not present in the transposase, indicating that GTP hydrolysis may or may not be involved in the complex DNA transposition reaction. To investigate the relationship between GTP-binding

activity and in vivo transposition of *Drosophila* P elements, Mul & Rio engineered the D379N mutation in P-element transposase (16).

Mul & Rio (16) used an elegant genetic screen involving excision of a P element from a reporter plasmid, which creates a functional kanamycin resistance gene to follow the activity of the transposase. With this cellular assay, many mutations affecting GTP binding were studied. Even though the P-element transposase does not contain the canonical GTP-binding motif, the D379N, which corresponds to the residues that can be mutated in the canonical GTPase sequences described above, somewhat surprisingly produced a transposase that accepts XTP rather than GTP. The D379N transposase mutant was then studied in insect cells, where transposition reactions could be scored by using the kanamycin resistance-based reporter assay. Strikingly, insect cells transfected with D279N transposase showed a 50-fold increase in DNA transposition when the cells were incubated with exogenous xanthosine. Xanthine could also be added extracellularly to induce transposition but afforded only one-half of the induction provided by xanthosine.

This elegant study demonstrated that the noncanonical GTP-binding motif of P-element transposase was quite similar, in terms of structure-function relationships, to other GTPases. Furthermore, Mul & Rio (16) used the XTPase mutation in transposase to demonstrate that nucleotide hydrolysis activity of this complex protein is essential for DNA transposition, through selective rescue of the cellular transposition function of D379N transposase by the addition of extracellular xanthosine to increase the intracellular concentration of XTP. It is important that Mul & Rio have shown that the addition of xanthosine in the medium of *Drosophila* Schneider L2 cells leads to an appreciable increase in intracellular XTP. This is in distinct contrast to the work of Yu et al (15), in which xanthosine treatment of COS cells did not produce a concentration of XTP to support G protein-coupled signaling. Either the G α_0 (mutant) signaling apparatus requires a higher concentration of XTP or the *Drosophila* cells possess a different balance of metabolic enzymes for controlling the GTP-GDP-XTP-XDP pools. In any case, this study demonstrates that not all in vivo cellular systems will react similarly to attempts at manipulation of intracellular nucleotide pools.

Because the GTPase family of enzymes represents one of the largest protein superfamilies in the genome, the XTPase mutation strategy promises to be a very valuable strategy for selectively manipulating one particular GTPase family in a complex mixture to carry out functional genomics studies of GTPases.

Seven-Transmembrane Receptors Activated Solely by Synthetic Ligands

The seven-transmembrane (7-TM) family of receptors is the largest family of transmembrane receptors in the human genome (17). They respond to photons, odorants, biogenic amines, lipids, peptide hormones, and other ligands. The 7-TM receptors control many physiological processes, including heart rate, proliferation, chemotaxis, neurotransmission, and hormone secretion (18). Ligand binding

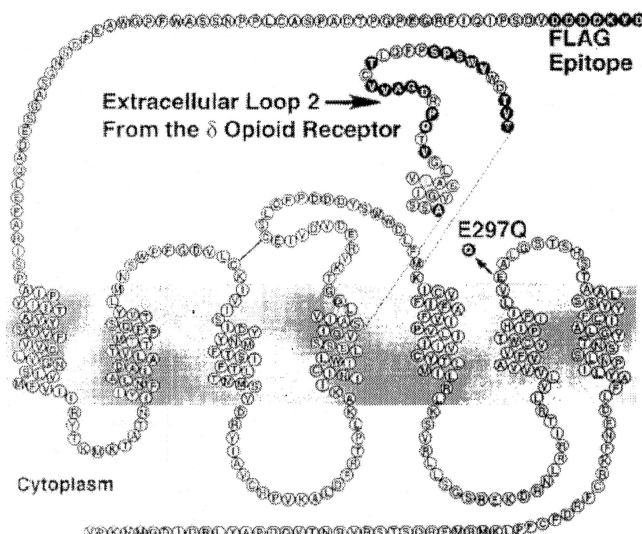


Figure 3 Topology of seven-transmembrane G protein-coupled receptor engineered to respond only to a synthetic ligand. The κ -opioid receptor is shown with a second extracellular loop transferred from the δ -opioid receptor to eliminate binding of endogenous ligands of the κ -opioid receptor.

induces dissociation of heterotrimeric (α , β , γ) G proteins, which are associated at the cytoplasmic side of the 7-TM receptors. As discussed above, $G\alpha s$ are induced to bind GTP rather than GDP when ligands bind to the receptor.

The 7-TM receptors represent the targets of an estimated 75% of current pharmaceuticals. Thus the repertoire of specific ligands for individual receptors is enormous and should allow for simple chemical control of any 7-TM receptor of interest. However, animal studies are complicated by the presence of endogenous peptide ligands, which can activate or inhibit signaling events. To get around the problem of endogenous activation of 7-TM receptors, Coward et al (19) have engineered receptors that respond only to synthetic ligands and not to their endogenous ligands.

The topology of 7-TM receptors is shown in Figure 3. The ligand-binding site is composed of contacts from the extracellular loops. Coward et al (19) capitalized on the fact that peptide hormone-binding contacts are distinct from the contacts made by small-molecule ligands. Specifically, peptides typically interact with the extracellular loops of the receptor, whereas small-molecule binding determinants are closer to the transmembrane domains.

Coward et al (19) engineered the well-characterized κ -opioid receptor to be unresponsive to endogenous ligands by swapping an extracellular loop from the δ -opioid receptor Ro1 (Figure 3). In addition, a point mutation was made in the first extracellular loop (E297Q). This site was known to contribute to specific peptide binding, because the cognate residue in the δ receptor is tryptophan (19). Furthermore, the E297A mutant in the κ -opioid receptor was known to disrupt

TABLE 4 κ -Opioid receptor and engineered RASSL (Ro2) affinity for the endogenous ligand dynorphin A and for two synthetic ligands, bremazocine and spiradoline^a

Ligand	Receptor	
	k-WT	Ro2
Dyn A(YGGFLRRIRPKLK)	0.06 ± 0.04	124.52 ± 19.38 (1946)
Bremazocine	0.04 ± 0.401	0.05 ± 0.02 (1.2)
Spiradoline	1.32 ± 0.38	5.65 ± 1.19 (4.3)

^aData are from 19. Data are expressed in nanomolar as mean ± SD. Fold differences from k-WT are shown in parentheses.

binding of κ -selective small-molecule agonists. To disrupt the essential chemical nature of the wild-type residue (Glu) to interfere with peptide hormone binding, without disruption of small-molecule binding, the conservative E297Q mutation was made, resulting in receptor Ro2. This engineered receptor displayed >2000-fold-lower binding affinity for the natural ligand dynorphin A (Table 4). Remarkably, however, the binding affinity for the synthetic ligand bremazocine was unchanged.

To test whether the engineered receptors could activate the expected downstream signaling pathways in cells, Ro1 and Ro2 were transfected into cells. Rat 1a cells proliferate in response to G_i signaling, which can be monitored easily as an increase in DNA synthesis (20). Wild-type κ -opioid receptor-transfected cells showed robust proliferation in response to the peptide hormone dynorphin A [50% effective concentration (EC₅₀) = 10 nM], whereas the engineered Ro1 induced no detectable proliferation, even at 100-fold-higher dynorphin A concentrations. The wild-type κ -opioid receptor and Ro1 showed the same levels of proliferation when stimulated with the synthetic ligand spiradoline [4.4 nM vs 5.5 nM, respectively (Figure 4A)]. Thus, the synthetic receptor Ro1 is insensitive to its natural ligand, yet can activate cellular responses when stimulated with synthetic agonists. Cell culture systems can demonstrate the feasibility of animal studies, yet many parameters that can be tightly controlled in cell culture are not manipulatable in an animal.

In an animal, it is difficult to determine a priori whether the receptors that are activated solely by synthetic ligands (RASSLs) will remain unstimulated, because of the many complicating factors in the in vivo production of peptide hormones. Redfern et al (21) directly addressed this question by engineering an Ro1-expressing transgenic mouse line.

To measure the effect of Ro1 expression in a whole animal, Redfern et al (21) used heart rate (HR) as a sensitive readout of RASSL responses. G_i signaling in the heart leads to a dramatic decrease in HR (bradycardia), which can be easily monitored (21). These authors engineered conditional and tissue-specific expression of Ro1 in mice. When Ro1 was expressed in the heart, where κ -opioid receptors are not expressed, the basal HR was 660, compared with a normal mouse HR of 650

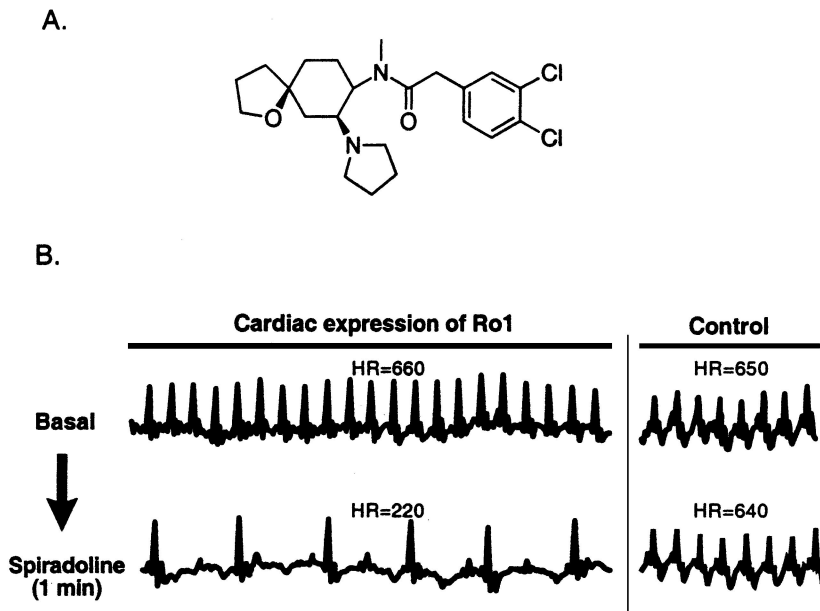


Figure 4 A. Chemical structure of spiradoline, a selective agonist of the κ -opioid receptor. B. Effect of spiradoline injection on heart rate of Ro1-expressing mouse vs control littermate that does not express Ro1 in the heart.

(Figure 4B). Thus, the 200-fold lowering of dynorphin A-binding affinity for Ro1 is sufficient to eliminate all stimulation of Ro1 by endogenous ligands.

When the synthetic ligand spiradoline was injected into the Ro1-transgenic mice, their HRs instantaneously (within <1 min) decreased to 220 (Figure 4B). The control mice that do not express Ro1 in the heart showed no bradycardia in response to spiradoline (HR, 640). Thus the RASSL engineered by Redfern et al (21) functioned perfectly in the whole-animal system, allowing for future investigations of a number of physiological and disease-related phenomena that are controlled by G_i-signaling pathways, including olfaction, taste transduction, weight control, memory, and locomotion.

In addition to the use of RASSLs to uncover the physiology of G protein-coupled receptors, Redfern et al (21) propose that RASSLs could be used to control physiologic responses with exogenously added ligands. The advantage to using RASSLs to control physiology is the rapidity of the G_i-coupled signal transduction cascade, allowing for induction of responses (<1 min) in contrast to other systems, which rely on dimerization (see below) or activation of transcription factors, which takes minutes or days, respectively.

Because spiradoline activates endogenous κ -opioid receptors, which are primarily expressed in the brain, the Ro1 transgenic system may be most useful

when used in conjunction with the recently produced κ -opioid receptor knockout mouse (22). This would allow the use of spiradoline to activate only the introduced Ro1 receptors and would be predicted to have no effect on G_i signaling in any tissue.

An alternative approach would be to further engineer RASSLs to respond to synthetic ligands, which are orthogonal to all endogenous G protein-coupled receptors. As pointed out by Redfern et al (21), such ligands have been developed, yet currently they are not sufficiently potent to use in animals. Perhaps the success of RASSLs in transgenic mice will encourage chemists to address this deficiency, allowing for RASSLs to be used ubiquitously without the need to knock out the endogenous κ -opioid receptors. The RASSL system not only is a success in terms of protein engineering but is also an extremely powerful method for deciphering the physiological consequences of stimulation of the >1000 predicted G protein-coupled receptors in the mouse genome.

Protein Kinases with Specificity for Unnatural Nucleotides

Protein kinases play a central role in controlling many diverse signal transduction pathways in all cells (24–26). These enzymes catalyze the phosphorylation of tyrosine, serine, or threonine residues on proteins by using ATP as the phosphodonor. The identification of the cellular substrates of individual protein kinases remains one of the central challenges in the field. We have recently developed a chemical method to tag the direct substrates of two Src family kinases, v-Src and Fyn (27, 28). To distinguish the substrates of v-Src from all other kinase substrates, we used structure-based design and site-directed mutagenesis to make v-Src catalyze a unique phosphotransfer reaction not catalyzed by any other protein kinase in the cell. We engineered the ATP-binding site of v-Src to uniquely accept an ATP analog (A*TP) as the phosphodonor substrate. The engineering of the active site of v-Src to accept [γ -³²P]A*TP provides a method by which the direct substrates of v-Src can be specifically radiolabeled in the presence of any number of cellular kinases (Figure 5, see color insert).

We have extended this strategy to a number of tyrosine and serine/threonine kinases to accept unnatural ATP analogs (28; Bishop AC, Shah K, Blethow J, Ubersax J, Morgan DO, Shokat KM, unpublished data). This was accomplished by using a semirational design approach. To create an orthogonal ligand, we synthesized N⁶-substituted derivatives of ATP (27). We then mutated a bulky residue in the active site of the kinase v-Src, Ile-338, to a smaller group, Ala or Gly. Ile-338 was chosen because it appeared to be in close contact with the N⁶ amine of ATP (Figure 6, see color insert). By screening a large panel of N⁶-substituted ATP analogs containing aliphatic or aromatic substituents, we identified the optimal A*TP substrates for the I338A and I338G mutated v-Src kinases.

Initially only the crystal structures of Ser/Thr kinases, protein kinase A (PKA), and cyclin dependent kinase 2 (CDK2) (29, 30) were available to guide our engineering of the tyrosine kinase v-Src. Crystal structures of PKA and CDK2, which

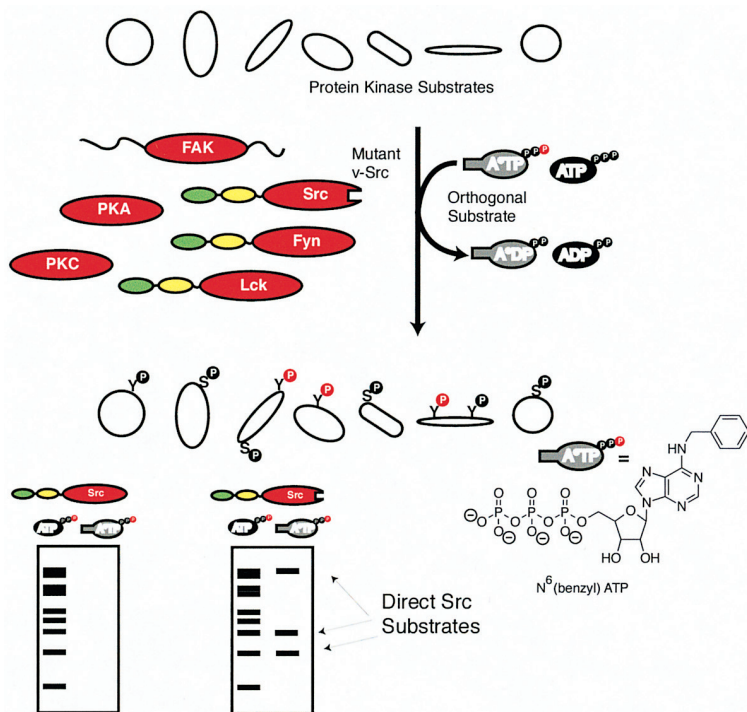


Figure 5 Chemical method of identifying direct downstream substrates of v-Src kinase. Red ovals represent the conserved kinase domain in different members of the protein kinase superfamily. Other ovals represent protein-protein association domains. Empty ovals represent cellular proteins which become phosphorylated by a variety of kinases. Ovals with a segment missing represent mutant kinases which accept “bumped” substrates such as N⁶(benzyl) ATP, as shown. Bottom rectangles represent hypothetical autoradiograms of protein gels to identify specific substrates of v-Src.

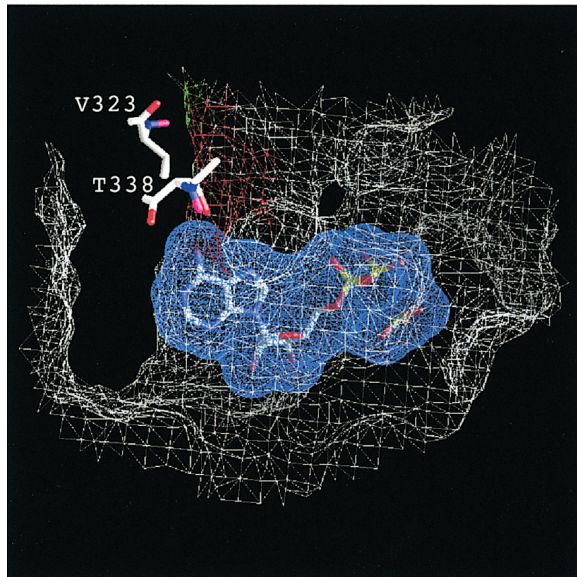


Figure 6 Surface representation of the ATP binding pocket in Hck, a Src-family tyrosine kinase. The solvent accessible surface of Kck within 7 Å of ATP is shown in *white* mesh, the surface of ATP is shown in *blue* mesh. The portion of Hck's solvent accessible surface area (A) formed by T338 (corresponding to L338 in v-Src) is colored *red* (mesh) and the portion of the surface formed by V323 is shown in *green* (mesh). ATP and residues T338 and V323 are shown in stick representation with the following atom coloring: O = *red*, N = *blue*, C = *white*, P = *yellow*. This figure was created using GRASP.

share only ~50% homology to v-Src, served as a limited guide to our design efforts. Based only on these structures, however, we introduced two mutations (V323A and I338A) into v-Src, affording a kinase with good specificity for N⁶ (cyclopentyl) ATP (27).

In the design of second-generation v-Src mutants, we were guided by newly solved structures of three tyrosine kinases—c-Src, Hck, and Lck (31–33). Relying heavily on the Hck-AMP-PNP cocrystal structure and kinase sequence alignments, we found that a single bulky residue at the position corresponding to Ile-338 in v-Src is primarily responsible for restricting the ability of wild-type kinases to accept N⁶-substituted ATP analogs. To our surprise, N⁶-(benzyl) ATP was the best substrate for the v-Src single mutation (*I338A* or *I338G*), based on screening a panel of >35 unique A*TP analogs (28; Shah K, Shokat KM, unpublished data). We had initially expected that an A*TP with a smaller substituent attached at the N⁶ position would better complement the small pocket engineered (Ile → Ala/Gly) into the kinase.

Although no crystal structure of the engineered v-Src kinase is yet available, several ligands bound to wild-type Src family kinases have been used to predict the binding mode of the orthogonal ATP analog, N⁶-(benzyl) ATP, to the engineered v-Src (34). From modeling studies, we conclude that, for the N⁶-substituted benzyl group to gain access to the existing pocket adjacent to N⁷, the side chain of residue 338 (a “molecular gate”) must be shortened (i.e. *I338A* or *G*). This analysis predicts that the benzyl ring of N⁶-(benzyl) ATP partially occupies a pocket already present in v-Src after the molecular gate, which normally restricts access to this pocket in all wild-type kinases, is removed by our mutation. This would explain why a larger than expected A*TP (>80 Å³) is the optimal analog identified in a screen of >35 A*TPs against *I338G* v-Src (28).

Further study of the binding mode suggested that more flexible links between the phenyl ring and the N⁶ amino group of ATP would allow better van der Waals packing of the added bump on the ligand into the engineered hole in the protein. It was suggested that one more methylene group could be added to the linker to allow the aromatic ring more flexibility to reach the existing pocket near the N⁷ atom of ATP.

In fact, the analog designed with an extra methylene group, N⁶-(2-phenethyl) ATP, is a better substrate ($k_{cat} = 0.6 \text{ min}^{-1}$; $K_m = 8 \mu\text{M}$ with I338A v-Src) than the previous optimal analog, N⁶-(benzyl) ATP [$k_{cat} = 0.5 \text{ min}^{-1}$; $K_m = 20 \mu\text{M}$ with the I338A mutant (28)]. For comparison, the kinetic constants for the I338A mutant with ATP are $k_{cat} = 1.0 \text{ min}^{-1}$ and $K_m = 70 \mu\text{M}$ (28). This confirms the prediction that adding extra flexibility into the substrate serves to orient the orthogonal substrate into the existing pocket above the N⁷ nitrogen.

To summarize, the binding site for orthogonal N⁶-substituted A*TP substrates of mutant v-Src proteins containing *I338A* or *I338G* mutations has been functionally probed with a wide variety of A*TPs. The pocket in the v-Src tyrosine kinase that accommodates the added substituents at the N⁶ position of ATP is actually present in the wild-type v-Src kinase. It is *access* to the existing pocket that is controlled

by Ile-338 in v-Src. Rather than engineering a new pocket by mutation of Ile to the smaller Ala or Gly residues, we believe that the *I338G* and *I338A* mutations provide a path for the N⁶ substituent on the ATP analog to gain access to an existing pocket in the ATP-binding site. Our laboratory has demonstrated that non-Src family tyrosine kinases, as well as many Ser/Thr-specific kinases, can be similarly engineered to accept N⁶-substituted ATP analogs including N⁶-(benzyl) ATP (Bishop AC, Blethrow J, Ubersax J, Morgan DO, Shokat KM, unpublished data).

Uniquely Inhibitable Protein Kinases

The ability to dissect signaling pathways by kinase substrate identification will certainly allow for more direct analysis of the roles of kinases in many diverse signaling environments. However, signaling pathways are not simply a summation of enzyme-substrate interactions. These pathways are highly interconnected, nonlinear, and exquisitely sensitive. Thus, in addition to biochemical mapping of pathways, genetic analyses of a pathway's organization provide important information about the key nodes of signal processing, by testing the functional importance of individual kinases. Unfortunately, because signaling cascades are responsible for ultrafast regulation of responses to light, oxygen, toxins, etc, genetic methods often fail to reveal the role of individual kinases because they are slow (days to weeks) at perturbing the system under study.

Regulation of kinase activity by homologous recombination in a mammalian genome requires at least 1–2 weeks even using the most sophisticated recombinase-mediated methods. During these 2 weeks, the signaling pathway of interest typically responds to the missing kinase by transcriptional up-regulation of a closely related kinase, which masks the real effect of missing the kinase of interest. A chemical method of inhibiting any kinase of interest would not suffer from such limitations, because small molecules can be added to the cell culture medium or the whole animal and in seconds bind to and inhibit the target.

Truly specific inhibitors for kinases and other members of large-protein super families are extremely difficult to identify. The stunning size and conserved active site fold of the protein kinase super family present two serious problems. First, the simple generation of a small-molecule inhibitor, which is unique for a single-family member out of a group of >2000 highly homologous proteins, is a daunting problem.

To rapidly develop uniquely specific inhibitors of any protein kinase in the genome, we have designed protein kinase inhibitors that inhibit only specifically mutated kinases. We have termed this approach the design of chemically sensitive alleles of protein kinases (35). To identify a cell-permeable small molecule that uniquely inhibits Ile-338–Gly v-Src, Bishop et al (35) tethered bulky chemical groups to the previously described Src family inhibitor, PP1 (36). Through modeling of the Src family-selective inhibitor PP1 (Figure 7, structure 1) in the active site of the Src family kinase Hck, it was predicted that PP1 would bind in an orientation analogous to that of ATP, therefore presenting its exocyclic amine (N⁴) to the space surrounding residue 338 (32). Thus, the amine was used as a chemical

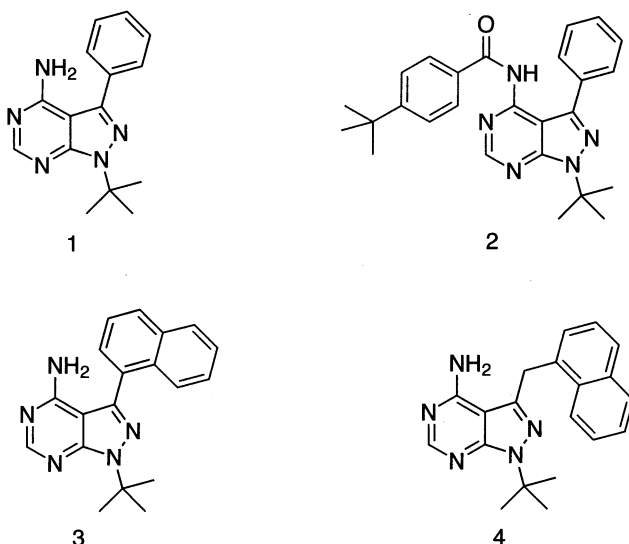


Figure 7 Chemical structures of PP-1, and its analogs which contain additional substituents (highlighted in blue bonds) designed to complement the additional space in appropriately mutated kinases.

hook to attach hydrophobic moieties that would prevent binding of the derivatized molecules to wild-type protein kinases. The same hook would concurrently generate novel van der Waals interactions with the engineered v-Src.

From a panel of 10 PP1 analogs, the most potent inhibitor of Ile-338-Gly was (4-[*p*-*tert*-butyl]benzamido-1-*tert*-butyl-3-phenylpyrazolo[3,4-*d*]pyrimidine) [50% inhibitory concentration (IC_{50}) = 430 nM; Figure 7, structure 2]. The selectivity of PP1 analog 2 was confirmed against wild-type v-Src, Fyn, Abl, PKA, and PKC- δ , all of which were inhibited \geq 700-fold less effectively than the target kinase. Bishop et al (35) also showed that the equivalent mutation in Fyn also made it sensitive to inhibition by PPI analog 2 ($IC_{50} = 830$ nM), showing that a chemical genetic approach to protein–small-molecule recognition can rapidly circumvent the selectivity problem inherent in the structural degeneracy of homologous protein families.

The use of kinase inhibitors, which are competitive with ATP, is complicated by the high intracellular concentrations of ATP (1–5 mM in most cell types). Pyrazolopyrimidine-based inhibitor 2 is highly selective for appropriately mutated kinases, yet lacks high potency. Typically 100- to 1000-fold increases in cellular EC_{50} values are found, compared with *in vitro* IC_{50} values for ATP-competitive kinase inhibitors. Thus, an inhibitor with an IC_{50} value of 400 nM will require 40–400 μ M in whole-cell assays, which is a concentration range in which general cytotoxicity can be induced.

To increase the potency of the pyrazolopyrimidine-based inhibitors, the binding mode of PP1 in the active site of the Src family kinase, Hck was investigated by

molecular modeling (32, 34). From this model, it was deduced that derivatization of N⁴ was not the only means of generating complementary van der Waals interactions with the unique binding pocket of I338G v-Src. It was predicted that derivatization of the C³ phenyl ring of PP1 [e.g. a phenyl ring replaced with a naphthyl ring system (Figure 7, PP1 analog 3)] with a bulky group leads to a steric clash between the derivatized inhibitor and the molecular surface created by Thr-338 (Figure 8, see color insert). Mutation of residue 338 to glycine generates a unique binding pocket, which is predicted to be large enough to accept the naphthyl analog of PP1. It was reasoned that derivatization of the phenyl group in PP1 with hydrophobic substituents should afford compounds that complement the corresponding I338G v-Src–active site, without disrupting any potential hydrogen-bonding interactions at N⁴. In addition, this added bulk at the C³ moiety should cause these molecules to be sterically incompatible with the active sites of wild-type tyrosine kinases, affording high specificity for the suitably engineered v-Src.

The group of modified inhibitors was screened against the catalytic domain of the target kinase, I338G v-Src, which was expressed in bacteria and purified as a glutathione-S-transferase (GST) fusion protein. All of the C³-derivatized analogs are more potent inhibitors of I338G v-Src than the most potent molecule (2, IC₅₀ = 430 nM) identified from the first-generation panel of N⁴ derivatized compounds (35). Two naphthyl analogs of PP1 (analogs 3 and 4) exhibited the greatest potency (IC₅₀ = 1.5 nM). Under the assay conditions, the parent molecule, PP1, inhibited its optimal target, Fyn, at only IC₅₀ = 30 nM. These data show that an inhibitor design strategy combining enzyme engineering with directed small-molecule synthesis could match the potency of molecules identified through screening of large libraries. Furthermore, this strategy can lead to a significant increase (20-fold analogs 3 and 4) in affinity over previously optimized inhibitors of wild-type kinases.

Identification of a selective enzyme inhibitor through chemical genetic design is useful only if the inhibitor can be used in a relevant cellular context to probe the target's function inside the cell. To demonstrate cellular inhibition of the target kinase by analog 3, Bishop et al (35) treated NIH 3T3 fibroblasts, which expressed either wild-type or Ile-338–Gly v-Src with the mutant-specific inhibitor (35). The mutant-selective inhibitor, PP1 analog 3, at 100 μM had no effect on the phosphotyrosine level of cells expressing wild-type v-Src, whereas the phosphotyrosine levels of cells that expressed the target kinase were moderately reduced. It is more striking that, under prolonged drug treatment, it was found that the Ile-338–Gly-expressing cells selectively reverted to the flattened morphology of nontransformed fibroblasts. This phenotype was confirmed by staining the actin stress fibers that are characteristic of normal fibroblasts (Figure 9, see color insert). No change in the morphology or actin organization was observed for the wild-type v-Src-expressing cells. Thus it was demonstrated that a small-molecule inhibitor, which is uniquely selective for a tyrosine kinase oncogene product, could revert the morphological changes associated with cellular transformation.

Only through chemical genetic design coupled with the built-in control of the wild-type target homolog could such a determination of cellular specificity be

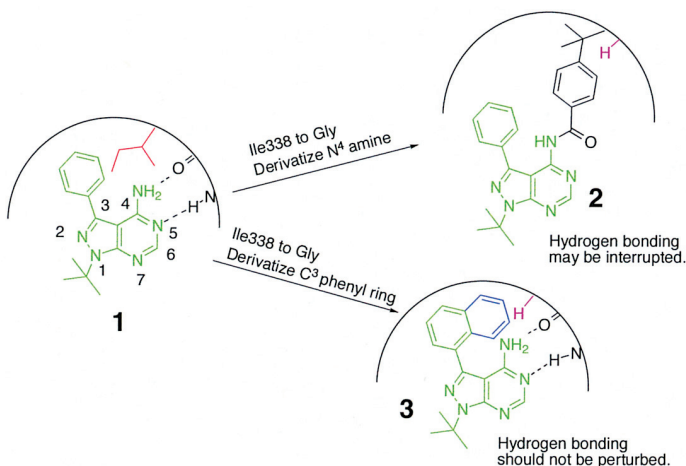


Figure 8 Schematic representation of the predicted binding orientation of two classes of derivatized prazolo[3,4-*d*]pyrimidines. Analogs that were derivatized at N⁴ may have lost potency due to an interruption of the ATP-like hydrogen bonding network. This network is presumably intact in the C³ derivatized inhibitors.

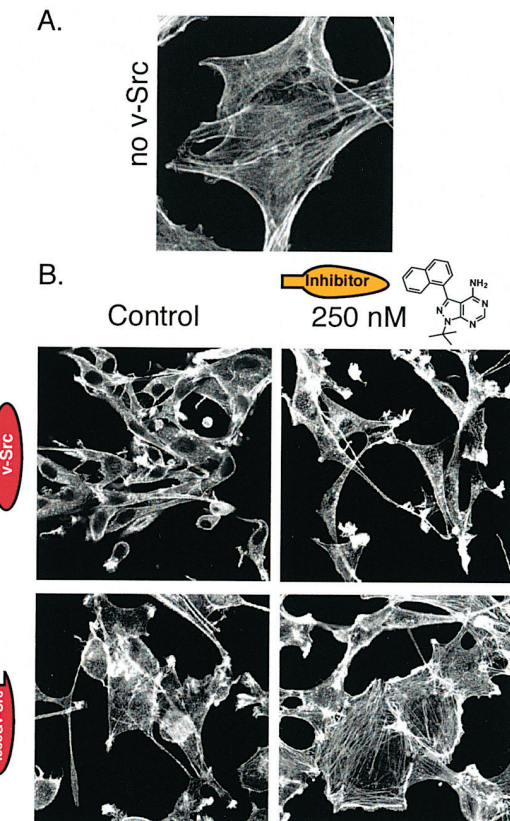


Figure 9 I338G v-Src transformed fibroblasts selectively acquire a flattened morphology and selectively regain actin stress fibers upon incubation with 3. (A) Non-transformed NIH3T3 cells. (B) Cells transformed by either wild-type v-Src or I338G v-Src were treated with 0.5% DMSO or 250 nM 3 in 0.5% DMSO for 16 hours. All cells were fixed, stained, with phalloidin-rhodamine, and visualized by confocal microscopy.

made. We have recently shown that PP1 analogs 2 and 3 are potent inhibitors of protein kinases in the Ser/Thr kinase super family, which are engineered to contain the same pocket, above the N⁶ position of ATP. This genome-wide approach to rapidly identifying potent small-molecule inhibitors of protein kinases will be useful for target validation of protein kinases as well as for generating adult knock-out-like phenotypes in transgenic animals.

Conditional Alleles of Kinesin and Myosin Motors

Another widely distributed family of ATP-utilizing enzymes is the motor protein family, including myosins and kinesins. Many different cellular processes are controlled by these force-generating enzymes, including muscle contraction, vesicle trafficking, cell motility, and axon guidance. To clarify the specific role of individual members of these families, two laboratories have developed mutant motors capable of interacting with unnatural ATP analogs to gain chemical control over individual motors in cells.

By making a space-creating mutation within the ATP-binding pocket of myosin 1 β , Gillespie et al have produced a mutant that is potently inhibited by particular bulky N⁶-substituted ADP analogs (37).

The actin-based myosin motor plays a crucial role in many specialized cellular events including extension of cellular processes (axonal outgrowth), cell division (cytokinesis), phagocytosis, signal transduction, cell movement, changes in cell shape during development, hearing, and muscle contraction (38). As many as 18 different myosin isoforms have been identified to date (Table 5). The myosin super family is divided into the conventional or type II myosins (those involved in muscle contraction) and the unconventional myosins (types I and III–XV+, as well as all other myosins). Features common to all myosin isoforms are a conserved

TABLE 5 Alignment of representative sequences from different classes of the myosin family (Genbank ID)

Class	Genbank ID	Sequence
RAT MYOSIN 1 β	(A45439) :	49 GSVVISVNPYRSLP .I ^Y SPEKVEDYRNRR 77
Class I:	P22467:	46 GPVLVSMNPYKQLG .I ^Y GNDQINLYKGKH 74
Class II:	P08964:	109 GLSLVAINPYHNLN .LYSEDHINLYHNKH 136
Class III:	P10676:	365 GDILLSLNSNEIKQ .EFPQEFLHAKYRFKS 384
Class V:	Q99104:	104 GIVLVAINPYEQQLP .I ^Y GEDIINAYSGQN 132
Class VI:	U49739:	91 ANILIAVNPYFDIPK ^I YSSDTIKSYQGKS 120
Class VII:	U81453:	99 GSILVAVNPYQLLS .I ^Y SPEHIRQYTNKK 127
Class VIII:	U94781:	151 GPVLVAINPFKKIP .LYGSDYIEAYKRKS 178
Class IX:	S54307:	180 GSILVAINPFKFLP .I ^Y NPKYVKMYENQQ 208
Class X:	U55042:	97 GSIIIASVNPYKTITGL ^L YSRDAVDRYSRCH 126
Class XI:	U94785	96 GNILIAINPFQRLPHLYDTHMMEQYKGAG 125

^aConserved tyrosine in rat myosin 1 β is highlighted. This residue can be mutated to glycine, allowing N⁶ substituted ATP analogs to be accepted as alternative substrates for mutant myosin 1 β .

head group that encompasses the actin-binding ATP-driven motor region, less-conserved domains involved in binding regulatory light-chain molecules, and divergent tail structures that likely provide specificity of function (e.g. binding of a particular cargo) (38).

Myosin binds to and moves along actin filaments in an ATP-dependent process. The hydrolysis of ATP within the myosin head group leads to the “ratcheting” of the head group, which charges it energetically to produce force upon return to the unratched state. It is in this bent state, bound to ADP and P_i , that myosin is capable of binding actin. Release of P_i leads to the unracheting of the actin-bound head group and the coincident movement of the myosin tail and its attached cargo towards the positive end of the actin filament. The release of ADP sets the stage for another cycle of ATP binding and hydrolysis. The binding of ATP releases the head group from actin. Release and rebinding of multiple myosin head groups provide the machinery by which myosin motors can move along an actin filament.

Several myosin isoforms have been implicated in the hearing process in mammals. MYO15, myosin VIIA, and myosin VI mutations all lead to apparent hearing loss in mice. Mutations in MYO15 and myosin VIIA have been mapped in deaf patients (39). Myosin isozyme expression studies (immunohistochemical techniques and *in situ* hybridization experiments) have provided insight into the potential players in certain aspects of hearing. However, given that multiple myosin isoforms are expressed in the auditory hair cells of the ear, direct proof of the role of a particular isozyme has been difficult. Developmental stresses put in place by the lack of one isozyme (as in knock-out mice) may result in the use of alternative isoforms, making genetic studies difficult to interpret.

Gillespie et al designed a system to probe the involvement of myosin 1 β in the hearing process. Making use of the knowledge that ADP release from myosin is the rate-limiting step in myosin movement along actin (i.e. in the presence of high concentrations of ADP, movement can be stalled), they have successfully designed isozyme-specific inhibitors of mutant myosin 1 β . Complementary space-creating and space-filling alterations in the conserved nucleotide-binding site of myosin 1 β and the nucleotide, respectively, have allowed allele-specific inhibition. Mutation of rat myosin 1 β tyrosine 61 (Figure 10) to glycine creates an enlarged binding pocket capable of uniquely accepting N⁶-substituted adenosine analogs. *In vitro* motility assays show that the mutant myosin is capable of functioning at or near wild-type levels in the presence of ATP and that its movement was inhibited robustly in the presence of N⁶-substituted ADP analogs. It is interesting that the mutant myosin motor actually moves more quickly ($0.12 \mu\text{m s}^{-1}$) than the wild-type motor ($0.03 \mu\text{m s}^{-1}$). This is caused by the lower ADP affinity of the Y61G mutant ($K_d = 74 \pm 19 \mu\text{M}$) compared with wild-type myosin ($K_d = 20 \pm 2 \mu\text{M}$). Because release of ADP is rate limiting for cycling of myosin (40), it is reasonable that the mutant with a space creating mutation in the adenine-binding site would move more quickly. The force generated by the mutant myosin would be predicted to be lower than that of the wild-type protein, but this has not been determined. It is important that the tyrosine mutated in myosin 1 β is

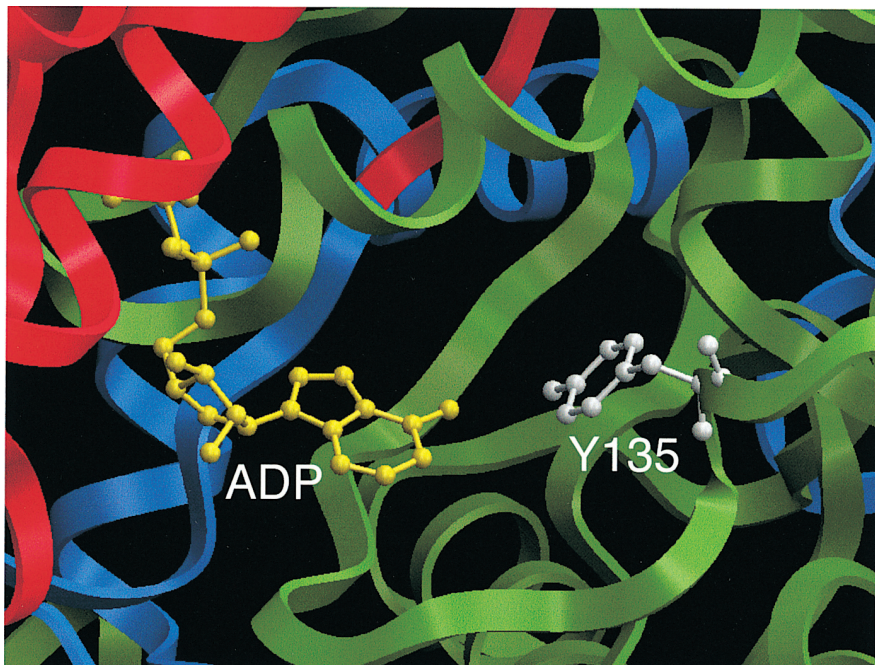


Figure 10 Myosin-I β Tyr-61 is a suitable residue for substitution. Ribbon representation of the Dictyostelium myosin-II motor domain complexed to ADP and aluminum fluoride. Note the close contact between adenine ring of ADP, shown in *yellow*, and Tyr-135 (Y135) equivalent to tyrosine-61 of rat or mouse myosin-I β , shown in *white*. The NH₂-terminal domain (25 kDa) is shown in *green*, the central domain (50 kDa) is shown in *red*, and the COOH-terminal domain (20 kDa in chicken skeletal muscle myosin) is shown in *blue*.

conserved across the myosin family, suggesting that the same strategy could be applied to other myosin family members.

The large kinesin super family of ATP-driven molecular motors have also proven amenable to a similar strategy for generating allele-specific inhibitors. Kinesin and kinesin-like proteins are responsible for movement of organelles along microtubules (MT), spindle formation, and the segregation of chromosomes at cell division (41). Kinesin super family members have a conserved MT-binding ATPase head group with structural similarities to the myosin head group (42). Kapoor and Mitchison examined of the amino acid residues within 5 Å of the ADP-N⁶ atom in the X-ray crystal structure of human kinesin (42) and noticed the presence of two conserved charged groups (Arg-14 and Arg-16).

Kapoor & Mitchison (43) have, in fact, recently reported the use of just such an approach to produce kinesin allele-specific activators and inhibitors. Mutation of Arg-14 to alanine does indeed provide a binding pocket, which is capable of using N⁶-cyclopentyl ATP. Not surprisingly, however, the removal of the charged group in the binding pocket disrupts the ability of the molecule to function with endogenous ATP, making the mutant kinesin reliant on the N⁶-substituted analog for its function (Table 6). Because hydrolysis of ATP, not release of ADP as in myosin, is the rate-limiting step in the kinesin system, Kapoor & Mitchison made use of a nonhydrolyzable form of the analog to specifically inhibit the mutant kinesin. Such allele-specific activators and inhibitors should allow the

TABLE 6 Engineered motor proteins kinesin and myosin, kinetic constants with ATP, and orthogonal nucleotides^a

	ATP					
	<i>K_m</i>	<i>V_{max}</i>	<i>K_m</i>	<i>V_{max}</i>		
kinesin	60 μM	0.6 μm/s	*	*	*	b
kinesin*	*	*	1200 μM	0.2 μm/s		
myosin1β	9–6 μM	0.5–0.3/s				230 μM
myosin1β*	10–2 μM	0.5–0.3/s				2.4 μM

*Very little activity.

^a*V_{max}* for kinesin is in microtuble movement (micrometers/second), whereas myosin results are given as ATP hydrolysis (1/s).

^bIn the presence of 25 μM actin and 10 μM ATP.

clarification of the role of individual kinesin family members in various cellular processes.

Conditional Alleles of Nuclear Hormone Receptors

The super family of nuclear hormone receptors is a unique family of transcriptional regulators. This group of receptors has both DNA-binding and ligand-dependent transactivation abilities. On selective binding of small-ligand molecules, this family of receptors can single-handedly provide a transcriptional signal to specific target genes (44).

The retinoid X receptor (RXR) activates the transcription of genes in response to 9-*cis*-retinoic acid (RA) or 9cRA, its natural ligand. Nuclear receptors such as RXR are a super family of ligand-inducible transcription factors that, along with RA receptors (RARs), play a role in the control of cellular differentiation and vertebrate development through their interaction with RAs. RAs are natural derivatives of vitamin A (retinol). The RXRs show a binding preference for 9-*cis*-RA whereas the RARs bind with equal affinity to 9-*cis* RA as well as to the stereoisomer, all-*trans*-RA (t-RA) (Figure 11).

RXR functions as a ligand-binding homodimer, but it is also able to function as a silent non-ligand-binding partner in a heterodimer with other nuclear receptors. Altered activation of nuclear hormone receptors in response to ligand binding occurs in natural and directed mutants and results in responses ultimately leading to diseased states. For example, a Thr-877→Ala mutation in the androgen receptor results in the inability to bind and activate in response to progesterone, estradiol, and antiandrogens (45). This mutation is associated with pharmacoresistant prostate cancer.

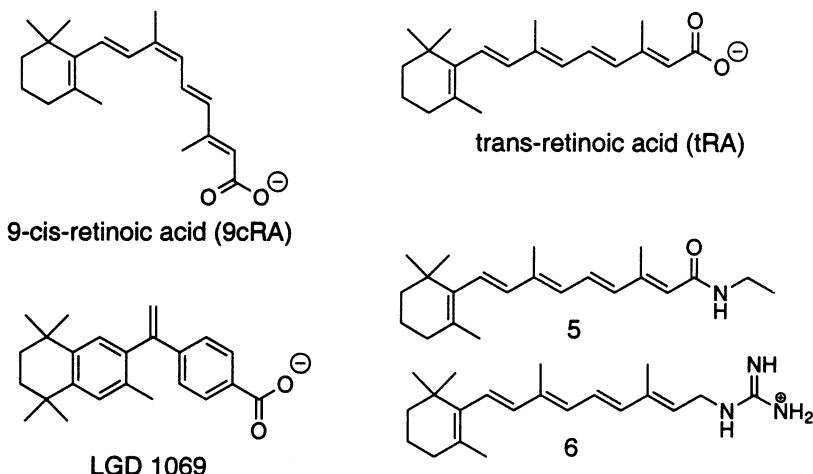


Figure 11 Chemical structures of 9-*cis*-retinoic acid (9cRA) and *trans*-retinoic acid (tRA) along with orthogonal ligands for engineered retinoic-acid receptors.

The development of receptors that could be activated by selected ligands would expand the applications for metabolic and genetic control, as well as provide insights into the structural specificity and origin of disease states. The ability to activate or repress transcription of specific genes by selective or “designer” ligands would provide a tool that is useful for the control of genetic and metabolic pathways.

Peet et al (46) tested a number of RXR synthetic ligands with a variety of RXR mutants, and this structure-based mutagenesis was used to change the ligand specificity of RXR. The amino acid residues Phe-313 and Leu-436 were found to be crucial in determining ligand specificity. The first class shows decreased activation by the natural ligand 9cRA and increased affinity for synthetic ligands. The second class continues to be activated by 9cRA but no longer responds to synthetic ligands (narrower specificity). Two new classes of mutant RXR proteins were developed.

Single and double mutants were tested in which Phe-313 and Leu-436 of RXR were changed to various uncharged amino acids. The Phe-313 → Ile mutation produced a dramatic shift in specificity—a 40-fold change in favor of the synthetic ligand LGD 1069 over the natural ligand 9cRA, as compared with the EC₅₀s of the wild-type RXR (Figure 11). The Phe-313 → Ala mutant also displayed a similar shift in specificity towards the synthetic ligands.

The only Leu-436 substitution to show any change in specificity was L436F. In contrast to the Phe-313 mutants, L436F shows a ninefold increase (less potent) in EC₅₀ for the natural ligand 9cRA, and a shift away from the synthetic ligands.

Koh and colleagues (47) investigated another member of the nuclear hormone receptor family (RAR γ) to selectively activate genes with small molecules designed to bind to engineered receptors. Specifically, the RAR γ was rationally reengineered to respond to novel synthetic ligands.

The crystal structure of t-RA in a complex with RAR γ was used for the design of the engineered receptor-synthetic and ligand pair (Figure 12, see color insert). Two residues were shown to interact directly with the carboxylic acid moiety of t-RA through site-directed-mutagenesis studies (48). These two residues (Ser-289 and Arg-278) possess the critical electrostatic and size recognition elements necessary for ligand binding. Mutation of one or both of these residues to glycine or to a negatively charged residue (Asp or Glu) results in receptors that prefer neutral or positively charged RA analogs such as ligands 5 and 6 (Figure 11). The synthetic analogs contain sterically larger groups or cationic groups in place of the carboxylic-acid moiety of t-RA. These ligand modifications complement the engineered receptors and are preferentially accepted by the mutants, compared with the wild type, with selectivities of >threefold between wild-type and mutant receptors (6) and 14.4-fold induction of the mutant receptor with ligand 5.

The ability to design and synthesize ligands for engineered nuclear hormone receptors opens up many exciting opportunities to study these complex transcription factors with small molecules. Examples of future directions may include the study of orphan nuclear hormone receptors, in which the natural ligand has

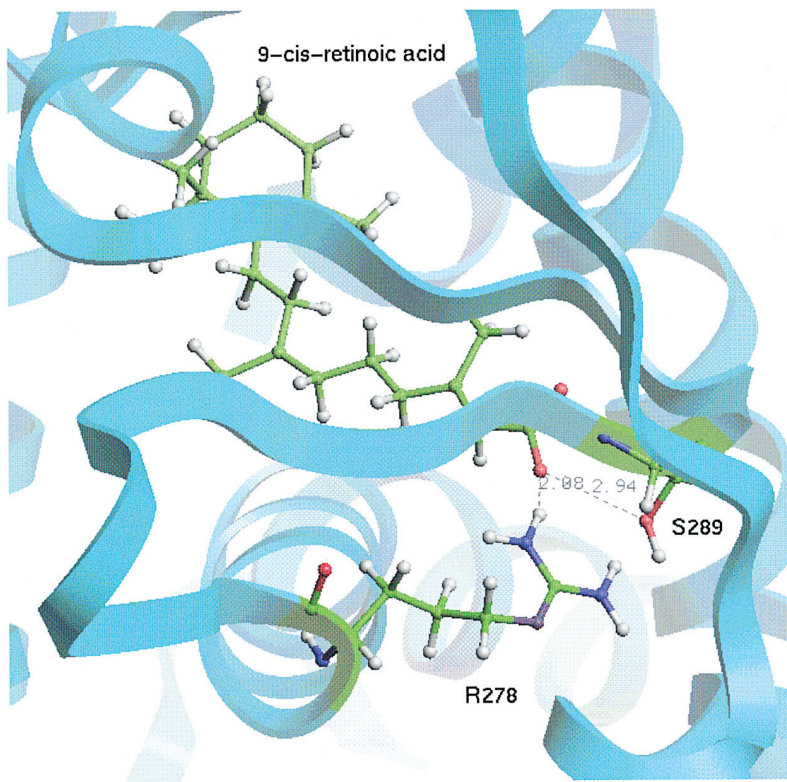


Figure 12 Ribbon diagram of 9-cis-retinoic acid bound to RAR γ . 9-cis-retinoic acid is shown in ball-and-stick representation as are the two key residues in RAR γ which form important contacts with the carboxylic acid of 9-cis-retinoic acid. Atom colors are the same as in Figure 1.

not been identified, or activation (agonist) of engineered receptors in transgenic animals.

ENGINEERING SIGNALING PATHWAYS FOR HUMAN THERAPY

Antibody-Directed Enzyme Prodrug Therapy

One of the major limitations of research strategies that use orthogonal-pair design is that they generally have little or no direct medicinally relevant applications in humans. Whereas the introduction of engineered proteins into a variety of lower organisms is now commonplace, modern medicine is still many years removed (technologically and ethically) from the generation of transgenic humans. However, Smith and co-workers (49) and Wolfe et al (50) have recently devised an elegant approach for using orthogonal enzyme/substrate pairs to selectively deliver potent cytotoxic agents to tumor cells *in vivo*.

It had previously been shown that antibody-directed enzyme prodrug therapy (ADEPT) can be used to deliver chemotherapeutic agents to tumors (51, 52). ADEPT is used to selectively target an enzyme of interest to a tumor by coupling the enzyme to a tumor-specific antibody. Generally, the selected enzyme catalyzes the cleavage of a prodrug to release the active drug in the vicinity of the tumor mass. Thus, a twofold treatment of the antibody-enzyme conjugate, followed by the small-molecule prodrug, could lead to potent cytotoxicity directed to tumor cells. Although such approaches to cancer therapy have great promise, they also face formidable hurdles. The introduction of foreign enzymes into the human bloodstream can be highly immunogenic. In addition, ADEPT therapies often show weak tumor cell selectivity because the prodrugs can be hydrolyzed by any number of wild-type enzymes in the patient.

Previous to the studies by Smith et al (49), Vitols et al (53) had developed an ADEPT system by using bovine carboxypeptidase A and prodrugs of the potent cytotoxic drug methotrexate (MTX). Smith et al set out to lower the immunogenicity and improve the target specificity of this system through orthogonal-pair design (49). Initially, the authors chose to use human carboxypeptidase A1 (hCPA1) to minimize the immune response from the introduction of a bovine enzyme. More importantly, they engineered hCPA1 so that it would be capable of hydrolyzing MTX prodrugs that were not substrates for either wild-type hCPA1 or hCPA2. To suitably engineer hCPA1, Christianson & Lipscomb used a model of the protein that had been generated by using the crystal structure of bovine carboxypeptidase A [CPA (54)]. To this protein they docked a model substrate and found that the side chain of Thr-268 of hCPA1 was in close contact with the 2 and 3 positions of the phenyl ring of substrates containing phenylalanine or tyrosine. Because it had been previously shown that MTX-Phe (7) was an excellent substrate for hCPA1 (53), the authors reasoned that derivatives of MTX-Phe with bulky substituents at the 2 or 3 positions should be uniquely accepted by mutants of hCPA1 that have smaller amino acids (glycine or alanine) at position 268.

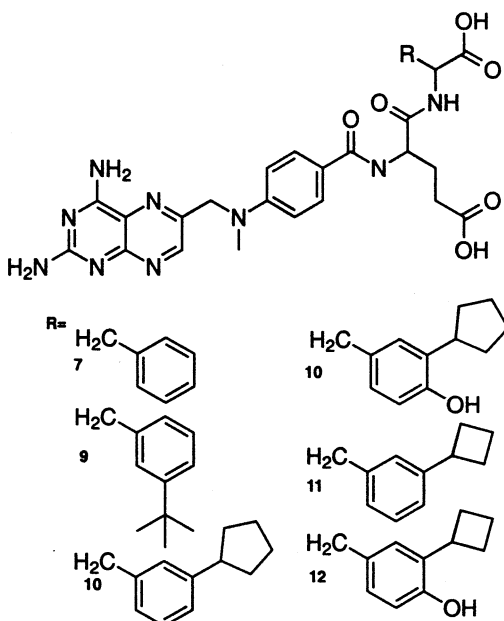


Figure 13 Chemical structures of orthogonal substrates for engineered carboxypeptidaseA designed to facilitate ADEPT (49).

Smith et al (49) synthesized a series of bulky aromatic MTX prodrugs, and, as would be expected, many of these molecules were extremely poor substrates for wild-type hCPA1 and hCPA2 (Figure 13) (49). In addition, these molecules were shown to possess far greater stability than MTX-Phe in pancreatic juice. The derivatized MTX prodrugs were then screened for their ability to act as substrates in hCPA1-T268G and hCPA1-T268A. The authors discovered that hCPA1-T268G was able to efficiently catalyze the hydrolysis of several of the bulky prodrugs (MTX-3-*t*-butyl-Phe-8, MTX-3-cyclopentyl-Phe-9, MTX-3-cyclopentyl-Tyr-10, MTX-3-cyclobutyl-Phe-11, and MTX-3-cyclobutyl-Tyr-12). Using the best substrate of the panel, MTX-3-cyclobutyl-Phe, hCPA1-T268G had a catalytic efficiency (k_{cat}/K_m) that was roughly fourfold higher than that of the wild-type enzyme with MTX-Phe and $>4 \times 10^5$ higher than MTX-3-cyclobutyl-Phe with wild-type hCPA1.

Smith et al (49) proceeded to demonstrate the utility of this system in a cell culture system by conjugating hCPA1-T268G to two separate antibodies. The enzyme was linked to ING-1, which recognizes Epcam, a protein expressed on many epithelial tumors, and to Campath-1H, which recognizes CDw52, which is expressed on the surface of lymphocytes (but not in epithelial cells). The antibody conjugates were incubated with the epithelial tumor cell line HT-29 at various concentrations to test for selective sensitization of the cells to the designed prodrug. It was found that preincubation with 10 $\mu\text{g}/\text{ml}$ of the ING-1-hCPA1-T268G conjugate strongly sensitized HT-29 cells to growth inhibition by

MTX-3-cyclobutyl-Phe and MTX-3-cyclopentyl-Tyr. At this conjugate concentration, the EC₅₀ was ~10 nM, which is roughly the same as with free MTX. In the absence of the antibody conjugate, the derivatized prodrugs were ~10³ less potent. As expected, in the presence of the Campath-1H-hCPA1-T268G conjugate, the sensitivity of HT-29 cells to the derivatized prodrugs was unchanged, demonstrating the immunospecificity of the ING-1-hCPA1-T268G ADEPT strategy.

In further studies, Wolfe et al (50) have investigated the *in vivo* efficacy of this orthogonal-pair ADEPT strategy in mouse models. Primary-toxicity studies showed that 8, 9, and 10 were highly stable *in vivo* and could be tolerated at doses 10- to 20-fold higher than free MTX. It was also shown that the ING-1-hCPA1-T268G conjugate localizes to tumor cells in Swiss nude mice bearing LS174T tumors. Over 144 h after injection, the tumor-to-blood ratio of the conjugate steadily grew to a maximum of 19.6. Despite these promising signs, however, treatment of the mice with the conjugate/prodrug therapy did not lead to a reduction of *in vivo* tumor growth for reasons that are to this point unclear.

Although, to date, it has not been shown that orthogonal MTX prodrugs will have an impact on the clinical treatment of cancer, the concept of heightening the specificity of ADEPT through orthogonal-pair design holds great promise. There are countless current and future prodrugs for which the general strategy of using a human enzyme to catalyze a “nonhuman” reaction could potentially prove applicable. The work of Smith and coworkers has demonstrated that medicinally important orthogonal pairs can possess enzymatic efficiencies that equal and surpass those of wild-type enzyme/substrate pairs. Ideally, in future approaches that combine ADEPT with orthogonal pairs, the oncology will correlate more strongly with the enzymology.

Initiation of Signals with Chemical Inducers of Dimerization

Because protein-protein interactions are key to almost all biological processes, a novel method for inducing intracellular protein dimerization was developed by Spencer et al (55). This method makes use of small, cell-permeable organic molecules called chemical inducers of dimerization (CIDs). CIDs have two binding surfaces that recognize one or more dimerization domains fused to target proteins. CID treatment causes the desired proteins to become cross-linked and initiate signaling. The protein complex can also be rapidly dissociated with the addition of a modified “CID,” having only one of the two binding surfaces. The dimerization domains were derived from immunophilins FKBP12, cyclophilin (CyP), and the FKBP12-rapamycin-binding domain of FKBP-rapamycin-associated protein (FRAP). Various CIDs have been used to initiate a wide array of signaling pathways by dimerizing receptors at the cell surface [e.g. insulin (56), platelet-derived growth factor (56), Fas (57, 58), erythropoietin (59), transforming growth factor (60), and T-cell antigen (61, 62)], to inducibly translocate cytosolic proteins to the plasma membrane [e.g. the GTP exchange factor Sos (61) and kinases such as Src (63), Lck, Zap70 (62), and Raf (64)], to import various proteins to (65) and export (66) them from the nucleus, to regulate gene transcription (67), to induce

cell-specific apoptosis, and to achieve regulated synthesis of human growth hormone in mice (68). CIDs have also been used to induce frog mesoderm in animal pole explants.

Initially, CIDs were either homodimers linked by a covalent tether of FK506 (FK1012) or cyclosporin (CsA)₂ or a heterodimer of FK506 and cyclosporin (FK-CsA). Complicating matters, FKBP12-FK506 complex binds to and inactivates calcineurin, a calcium-calmodulin-dependent protein phosphatase (69). This binding causes impaired signaling of the T-cell receptor followed by immunosuppression and toxicity. Therefore, these CIDs were modified synthetically to counteract their intrinsic biological activities.

Although the control of various signal transduction events with the CIDs has proven to be versatile, a significant shortcoming of this approach is the poor specificity of CIDs towards the wild-type immunophilins. The high expression of immunophilins in cells reduces the potency of CID ligands toward immunophilin fusion proteins by forming nonspecific receptor-ligand complexes. In transgenic animals, where there may be few cells expressing the desired fusion protein, the abundance of natural immunophilin could mask the biological response to CIDs. To improve the specificity of these CIDs, the orthogonal-pair or “bump-hole” strategy was developed.

The CIDs were modified to contain bulky substituents that clash with the amino acid side chains in the receptor, thereby abolishing its binding with wild-type receptors. Complementary mutations were made in the receptor that restores binding to these modified CIDs. Initially, cyclophilin-cyclosporin (CyP-CsA) was used as a model system to make this unique receptor-ligand pair (70). The crystal structure of the CyP-CsA complex revealed a hydrophobic interaction between the side chain of MeVal11 of CsA and a pocket of the CyP receptor. A modified CsA ligand was synthesized, in which the addition of only a methyl group to MeVal11 was enough to reduce the binding affinity from K_d from 5 nM to >3 mM with the wild type (Figure 14). As such, four different complementary mutations were rationally designed in the immunophilin receptor. The double mutant CyP(S99T, F113A) with modified CsA (MeIle11) showed >1000-fold selectivity ($K_d \sim 2$ nM). Although in the NFAT-signaling assay, MeIle11-CsA potently inhibited NFAT signaling in cells expressing CyP(S99T, F113A), MeIle11-CsA also caused the same inhibition in the cells expressing wild-type CyP ($IC_{50} \sim 300$ nM). To further improve this specificity, a more orthogonal CsA analog (CsA*) was synthesized that substituted a cyclopentylsarcosine (Figure 14) for the MeVal11 side chain. This compound does not bind CyP ($K_d > 15 \mu\text{M}$) and thus does not inhibit calcineurin in the wild-type cells. However, CsA* binds to triple-mutant CyP (F113G, C115M, S99T; CyP*) with very high affinity ($K_d \sim 9$ nM). Thus, this orthogonal receptor-ligand pair provides a potent tool for calcineurin inhibition in a cell- or tissue-specific manner.

The orthogonal design strategy was also extended to the rapamycin-FRAP system. Rapamycin binds to both FKBP12 and the FKBP12-rapamycin-binding domain of FRAP simultaneously to inhibit the activation of p70 S6 kinase and cyclin-dependent kinases (71). To study the role of FRAP in this pathway, a bump

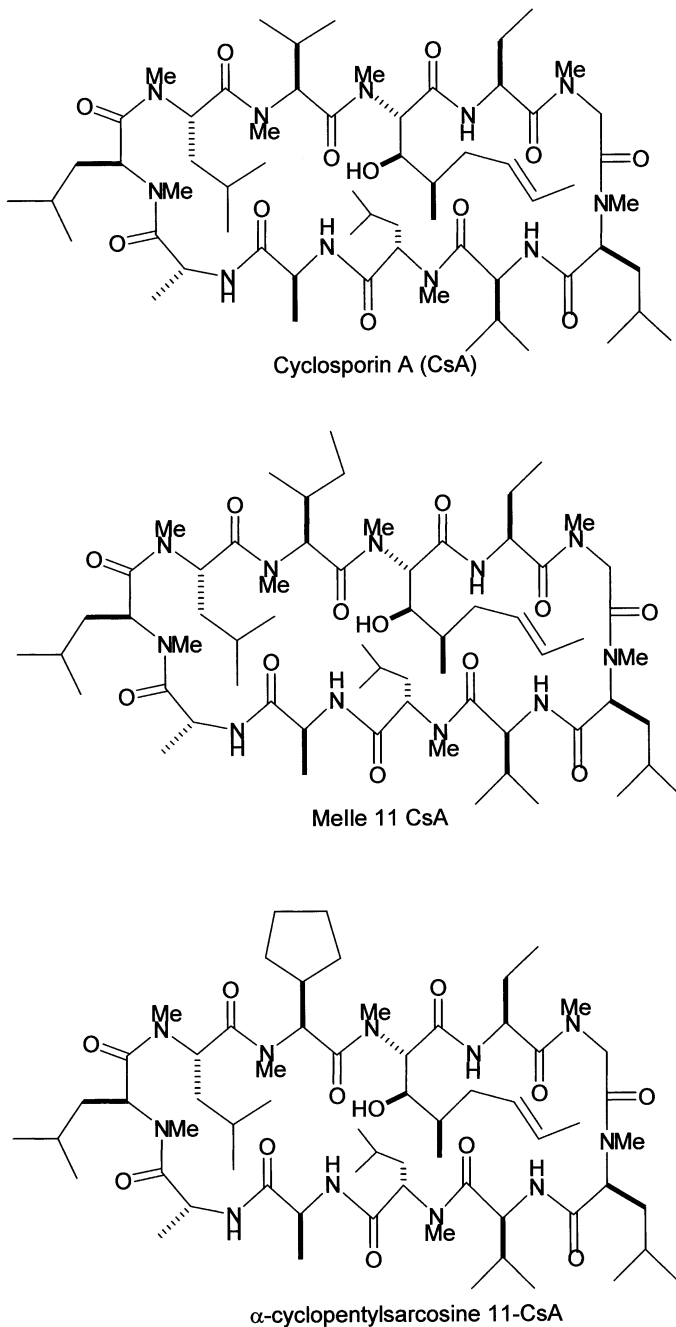


Figure 14 Chemical structures of cyclosporin A (CsA) and two analogs of CsA: Melle 11 CsA, α -cyclopentylsarcosine 11-CsA, designed to complement specifically engineered cyclophilin proteins. Atoms which were added to CsA to preclude binding to wild-type cyclophilin are highlighted.

was added to the FRAP protein by mutating Ser-2035 to either threonine or an isoleucine. The orthogonal FRAP mutants did not bind the FKBP12-rapamycin complex and were used to explore its cellular function after inhibiting the endogenous FRAP with rapamycin. This system revealed that inhibition of FRAP blocks signaling to p70 S6 kinase and 4E-BP, thereby interfering with the translation of specific messenger RNA transcripts and G1 cell cycle progression.

To prevent rapamycin from inhibiting cell proliferation, nontoxic dimerizers (rapamycin*) were synthesized with a bulky substituent at the C16 position. Both methallyl and isopropoxy substituents at this position abrogated rapamycin* binding to FRAP and allowed T-cell proliferation (72). To identify compensating holes, a triple mutant of FRAP was tested that restored its ability to bind one of the rapamycin* ligands (from 500 to 10 nM). As a result, Liberles et al (72) were able to induce targeted gene expression in Jurkat T cells with an EC₅₀ of <10 nM, by using this orthogonal pair.

Clackson et al redesigned the FKBP-ligand interface to introduce a novel specificity-binding pocket (73). The crystal structure of a high-affinity synthetic ligand of FK506 (FKBP ligand 1) with FKBP revealed that the C9 carbonyl group packs tightly against Tyr-26 and Phe-36 of FKBP (Figure 15a, see color insert). Therefore C9 carbonyl was replaced by larger ethoxy or ethyl group that selectively abrogated its binding to the wild-type protein ($K_d > 10 \mu\text{M}$). To rescue the binding of the orthogonal ligand with FKBP, four different mutants were tested containing different point mutations at Phe-36. All of these mutants restored binding and preferred *S* stereoisomers over *R* at the C9 position. To further improve the specificity of the *S*-ethyl-modified ligand, a trimethoxyphenyl group was used to replace the branched aliphatic side chains at this position. This resulted in a highly specific ligand ($K_d \sim 0.1 \text{ nM}$), which is 1000-fold more specific for FKBP (F36V) than the wild-type protein.

Clackson and coworkers (73) have studied the interaction between engineered (F36V) FKBP and the orthogonal ligands with high resolution by using X-ray crystallography. The crystal structure, solved at 1.9-Å resolution (Figure 15b), is the first crystal structure of an engineered receptor ligand pair, and it provides tremendous insight into the critical design considerations necessary to achieve high-selectivity ligands for engineered receptors.

The first question answered by this structure relates to the compensatory changes in the protein that occur in response to the space-creating mutation. The structure of F36V shows that there are essentially no compensatory structural adjustments to the rest of FKBP. Furthermore, the F36V mutation opens up an additional 90 Å³ of volume in the active site (Figure 15b).

Analysis of the binding conformation of the engineered ligand exactly agreed with the predictions in terms of the stereochemical preference for attachment of the ethyl group to FK506. The most interesting feature of the cocrystal structure is the failure of the ethyl bump to completely fill the introduced hole in the kinase. A completely enclosed cavity of ~60 Å³ is left unoccupied in the cocrystal structure.

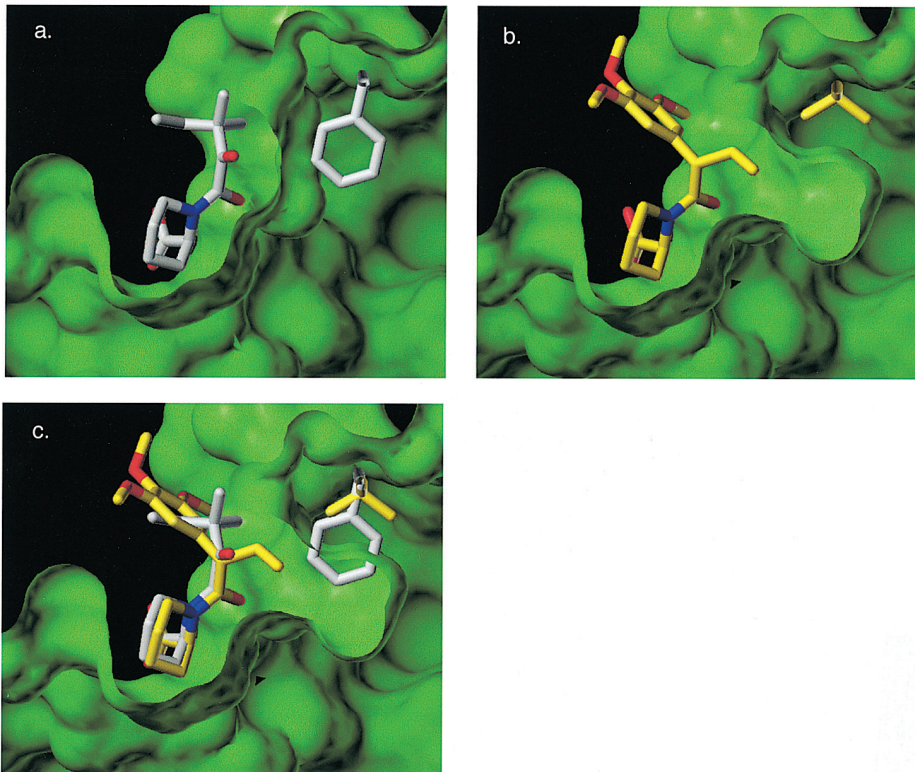


Figure 15 Crystal structure of a remodeled interface between the FK506-binding protein (FKBP) and a synthetic ligand. A cutaway through the solvent-accessible area is shown (green); carbon atoms of the original complex are shown in white and those of the modified complex are in yellow. (a) The complex between wild-type FKB and a synthetic ligand, showing the tight complementarity around the C9 carbonyl group. The sidechain of Phe36 is shown. This interaction has a K_d of 10 nM. (b) Complex of a ligand with a designed C9 S-ethyl bump with F36V FDBP. Apart from the removal of the Phe36 sidechain, the protein structure is essentially identical to that of the wild type. Note that the bumped ligand also has a second difference compared to the ligand in (a); a C9 trimethoxy substituent was substituted in place of tert-pentyl to improve affinity. This interaction has a K_d of 0.1 nM. (c) Overlay of (a) and (b). For further details see (1, 73).

Furthermore, no ordered water molecules were visible in the structure, suggesting that the remaining void is not occupied by solvent.

The remaining space in the cocrystal structure actually suggests something more broadly for engineering of orthogonal-receptor ligand pairs. Even with imperfect filling of the engineered pocket, it appears that high-affinity interactions can be recapitulated. One way to interpret this result is to realize that the way in which such ligands are discovered is first by discovery of an optimal “unbumped” ligand. This unbumped ligand provides many highly specific H-bond and van derWaals interactions with the protein target. The addition of a bump to this ligand can easily remove its ability to bind the protein (orthogonality). However, when a compensating hole is introduced into the protein, all of the formerly optimized interactions of the ligand with the protein can be regained by simply removing the steric insult of the added bump. In addition, the added bump and hole can create a greater surface area for interaction, which allows for even tighter binding than the original optimized situation.

The engineered FKBP (F36V) has been used in a wide variety of cell contexts to control diverse signaling pathways. A chimeric protein, FKBP (F36V) fused to the intracellular domain of the Fas receptor was expressed both in cells and in mice. Treatment of the modified ligand AP1903 caused rapid apoptosis of the engineered cells and in a mouse model, independently of endogenous FKBP.

Thus, the reengineering of the protein-ligand interface allows unparalleled temporal control of gene expression and protein subcellular localization that can be used for therapeutic purposes in the presence of endogenous proteins.

CONCLUSIONS AND FUTURE DIRECTIONS

The ability to genetically program individual proteins in cells or whole organisms for inhibition by small organic molecules should continue to provide highly specific information about the role of key proteins in complex signal transduction pathways. The rapid increase in the number of drug targets identified through genomic approaches could be validated by using such combined chemical and genetic techniques.

Further structural studies of engineered receptors and orthogonal ligands also promise to provide interesting insights into the key design features required of such engineered interfaces.

ACKNOWLEDGMENTS

We thank the following funding agencies for supporting our early work on engineered kinases: National Science Foundation MCB-9874587, National Institutes of Health (R01 CA70331-04, IROIAI/CA44009-01), Pew Charitable Trust, Searle Foundation, Cottrell Scholars Program, and GlaxoWellcome. We are also especially grateful to Tim Clackson and Bruce Conklin for providing Figures 3, 4, and 14, describing their work.

Visit the Annual Reviews home page at www.AnnualReviews.org

LITERATURE CITED

- Clackson T. 1998. *Curr. Opin. Struct. Biol.* 8:451–458
- Crews CM, Splittergerber U. 1999. *Trends Biochem. Sci.* 24:317–20
- Schreiber SL. 1998. *Bioorg. Med. Chem.* 6:1127–52
- Hwang Y-W, Miller DL. 1987. *J. Biol. Chem.* 262:13081–85
- Weijland A, Parlato G, Parmeggiani A. 1994. *Biochemistry* 33:10711–17
- Powers T, Walter P. 1995. *Science* 269 (5229):1422–24
- Jones S, Litt RJ, Richardson CJ, Segev N. 1995. *J. Cell Biol.* 130:1051–61
- Weis K. 1998. *Trends Biochem. Sci.* 23:185–89
- Sweet DJ, Gerace L. 1996. *J. Cell Biol.* 133:971–83
- Weis K, Dingwall C, Lamond AI. 1996. *EMBO J.* 15:7120–28
- Zhong JM, Chen-Hwang MC, Hwang YW. 1995. *J. Biol. Chem.* 270:10002–7
- Feig LA, Pan BT, Roberts TM, Cooper GM. 1986. *Proc. Natl. Acad. Sci. USA* 83:4607–11
- Schmidt G, Lenzen C, Simon I, Deuter R, Cool RH, et al. 1996. *Oncogene* 12:87–96
- Cool RH, Schmidt G, Lenzen CU, Prinz H, Vogt D, Wittinghofer A. 1999. *Mol. Cell Biol.* 19:6297–305
- Yu B, Slepak VZ, Simon MI. 1997. *J. Biol. Chem.* 272:18015–19
- Mul YM, Rio DC. 1997. *EMBO J.* 16:4441–47
- Strader CD, Fong TM, Tota MR, Underwood D, Dixon RA. 1994. *Annu. Rev. Biochem.* 63:101–32
- Spiegel AM, Shenker A, Weinstein LS. 1992. *Endocrinol. Rev.* 13:536–65
- Coward P, Wada HG, Falk MS, Chan SD, Meng F, et al. 1998. *Proc. Natl. Acad. Sci. USA* 95:352–57
- Pace AM, Wong YH, Bourne HR. 1991. *Proc. Natl. Acad. Sci. USA* 88:7031–35
- Redfern CH, Coward P, Degtyarev MY, Lee EK, Kwa AT, et al. 1999. *Nat. Biotechnol.* 17:165–69
- Simonin F, Valverde O, Smadja C, Slowe S, Kitchen I, et al. 1998. *EMBO J.* 17:886–97
- Strader CD, Gaffney T, Sugg EE, Candelore MR, Keys R, et al. 1991. *J. Biol. Chem.* 266:5–8
- Pawson T. 1995. *Nature* 373:573–80
- Cohen GB, Ren R, Baltimore D. 1995. *Cell* 80:237–48
- Hunter T. 1995. *Cell* 80:225–36
- Shah K, Liu Y, Deirmengian C, Shokat KM. 1997. *Proc. Natl. Acad. Sci. USA* 94:3565–70
- Liu Y, Shah K, Yang F, Witucki L, Shokat KM. 1998. *Chem. Biol.* 5:91–101
- Zheng J, Knighton DR, Ten Eyck LF, Karlsson R, Zuong N-H, et al. 1993. *Biochemistry* 32:2154–61
- Jeffrey PD, Russo AA, Polyak K, Gibbs E, Hurwitz J, et al. 1995. *Nature* 376:313–20
- Xu W, Harrison SC, Eck MJ. 1997. *Nature* 385:595–602
- Sicheri F, Moarefi I, Kuriyan J. 1997. *Nature* 385:602–9
- Yamaguchi H, Hendrickson WA. 1996. *Nature* 384:484–89
- Liu Y, Shah K, Yang F, Witucki L, Shokat KM. 1998. *Bioorg. Med. Chem.* 6:1219–26
- Bishop AC, Shah K, Liu Y, Witucki L, Kung C, Shokat KM. 1998. *Curr. Biol.* 8:257–66
- Hanke JH, Gardner JP, Dow RL, Changelian PS, Brissette WH, et al. 1996. *J. Biol. Chem.* 271:695–701
- Gillespie PG, Gillespie SKH, Mercer JA, Shah K, Shokat KM. 1999. *J. Biol. Chem.* 274:31378–81
- Karp G. 1996. *Cell and Molecular Biology: Concepts and Experiments*. New York: John Wiley & Sons

39. Redowicz M. 1999. *J. Muscle Res. Cell Motil.* 20:241–48
40. Spudich JA. 1994. *Nature* 372:515–18
41. Hirokawa N. 1998. *Science* 279:519–26
42. Kull FEA. 1996. *Nature* 380:550–55
43. Kapoor T, Mitchison T. 1999. *Proc. Natl. Acad. Sci. USA* 96:9106–11
44. Weatherman R, Fletterick R, Scanlan T. 1999. *Annu. Rev. Biochem.* 68:559–81
45. Veldscholte J, Ris-Stalpers C, Kuiper GG, Jenster G, Berrevoets C, et al. 1990. *Biochem. Biophys. Res. Commun.* 173:534–40
46. Peet DJ, Doyle DF, Corey DR, Mangelsdorf DJ. 1998. *Chem. Biol.* 5:13–21
47. Koh J, Putnam M, Tomic-Canic M, McDaniel C. 1999. *J. Am. Chem. Soc.* 121:1984–85
48. Tairis N, Gabriel JL, Soprano KJ, Soprano DR. 1995. *J. Biol. Chem.* 270:18380–87
49. Smith GK, Banks S, Blumenkopf TA, Cory M, Humphreys J, et al. 1997. *J. Biol. Chem.* 272:15804–16
50. Wolfe LA, Mullin RJ, Laethem R, Blumenkopf TA, Cory M, et al. 1999. *Bioconjug. Chem.* 10:38–48
51. Sell S, Reisfeld RA. 1985. *Monoclonal Antibodies in Cancer*. Clifton, NJ:Human Press
52. Huennekens FM. 1994. *Adv. Enzyme Enzym. Regul.* 34:397–419
53. Vitols KS, Haag-Zeino B, Baer T, Montejano YD, Huennekens FM. 1995. *Cancer Res.* 55:478–81
54. Christianson DW, Lipscomb WN. 1989. *Acc. Chem. Res.* 22:22–69
55. Spencer DM, Wandless TJ, Schreiber SL, Crabtree GR. 1993. *Science* 262:1019–24
56. Yang J, Symes K, Mercola M, Schreiber SL. 1998. *Curr. Biol.* 8:11–18
57. Spencer DM, Belshaw PJ, Chen L, Ho SN, Randazzo F, et al. 1996. *Curr. Biol.* 6:839–47
58. Belshaw PJ, Spencer DM, Crabtree GR, Schreiber SL. 1996. *Chem. Biol.* 3:731–38
59. Blau CA, Peterson KR, Drachman JG, Spencer DM. 1997. *Proc. Natl. Acad. Sci. USA* 94:3076–81
60. Stockwell BR, Schreiber SL. 1998. *Chem. Biol.* 5:385–95
61. Holsinger LJ, Spencer DM, Austin DJ, Schreiber SL, Crabtree GR. 1995. *Proc. Natl. Acad. Sci. USA* 92:9810–14
62. Graef IA, Holsinger LJ, Diver S, Schreiber SL, Crabtree GR. 1997. *EMBO J.* 16:5618–28
63. Spencer DM, Graef I, Austin DJ, Schreiber SL, Crabtree GR. 1995. *Proc. Natl. Acad. Sci. USA* 92:9805–9
64. Farrar MA, Alberol I, Perlmutter RM. 1996. *Nature* 383:178–81
65. Belshaw PJ, Ho SN, Crabtree GR, Schreiber SL. 1996. *Proc. Natl. Acad. Sci. USA* 93:4604–7
66. Klemm JD, Beals CR, Crabtree GR. 1997. *Curr. Biol.* 7:638–44
67. Ho SN, Biggar SR, Spencer DM, Schreiber SL, Crabtree GR. 1996. *Nature* 382:822–26
68. Rivera VM, Clackson T, Natesan S, Pollock R, Amara JF, et al. 1996. *Nat. Med.* 2:1028–32
69. Liu J, Farmer JD Jr, Lane WS, Friedman J, Weissman I, Schreiber SL. 1991. *Cell* 66:807–15
70. Belshaw PJ, Schoepfer JG, Liu K-Q, Morrison KL, Schreiber SL. 1995. *Angew. Chem. Int. Ed. Engl.* 34:2129–2132
71. Brown EJ, Beal PA, Keith CT, Chen J, Shin TB, Schreiber SL. 1995. *Nature* 377:441–46
72. Liberles SD, Diver ST, Austin DJ, Schreiber SL. 1997. *Proc. Natl. Acad. Sci. USA* 94:7825–30
73. Clackson T, Yang W, Rozamus LW, Hatada M, Amara JF, et al. 1998. *Proc. Natl. Acad. Sci. USA* 95:10437–42
74. Kang C, Sun N, Honzatko RB, Fromm HJ. 1994. *J. Biol. Chem.* 269:24046–24049
75. Maier T, Lottspeich F, Bock A. 1995. *Eur. J. Biochem.* 230:133–38
76. Barbieri MA, Hoffenberg S, Roberts R, Mukhopadhyay A, Pomrehn A, et al. 1998. *J. Biol. Chem.* 273:25850–55



CONTENTS

MEASURING THE FORCES THAT CONTROL PROTEIN INTERACTIONS, <i>Deborah Leckband</i>	1
STRUCTURE AND FUNCTION OF LIPID-DNA COMPLEXES FOR GENE DELIVERY, <i>S. Chesnay, L. Huang</i>	27
SIGNALING AND SUBCELLULAR TARGETING BY MEMBRANE-BINDING DOMAINS, <i>James H. Hurley, Saurav Misra</i>	49
GCN5-RELATED N-ACETYLTRANSFERASES: A Structural Overview, <i>Fred Dyda, David C. Klein, Alison Burgess Hickman</i>	81
STRUCTURAL SYMMETRY AND PROTEIN FUNCTION, <i>David S. Goodsell, Arthur J. Olson</i>	105
ELECTROKINETICALLY CONTROLLED MICROFLUIDIC ANALYSIS SYSTEMS, <i>Luc Bousse, Claudia Cohen, Theo Nikiforov, Andrea Chow, Anne R. Kopf-Sill, Robert Dubrow, J. Wallace Parce</i>	155
DNA RECOGNITION BY Cys2His2 ZINC FINGER PROTEINS, <i>Scot A. Wolfe, Lena Nekludova, Carl O. Pabo</i>	183
PROTEIN FOLDING INTERMEDIATES AND PATHWAYS STUDIED BY HYDROGEN EXCHANGE, <i>S. Walter Englander</i>	213
QUANTITATIVE CHEMICAL ANALYSIS OF SINGLE CELLS, <i>D. M. Cannon Jr, N. Winograd, A. G. Ewing</i>	239
THE STRUCTURAL BIOLOGY OF MOLECULARrecognition BY VANCOMYCIN, <i>Patrick J. Loll, Paul H. Axelsen</i>	265
COMPARATIVE PROTEIN STRUCTURE MODELING OF GENES AND GENOMES, <i>Marc A. Martí-Renom, Ashley C. Stuart, András Fiser, Roberto Sánchez, Francisco Melo, Andrej Sali</i>	291
FAST KINETICS AND MECHANISMS IN PROTEIN FOLDING, <i>William A. Eaton, Victor Muñoz, Stephen J. Hagen, Gouri S. Jas, Lisa J. Lapidus, Eric R. Henry, James Hofrichter</i>	327
ATOMIC FORCE MICROSCOPY IN THE STUDY OF MACROMOLECULAR CRYSTAL GROWTH, <i>A. McPherson, A. J. Malkin, Yu. G. Kuznetsov</i>	361
A DECADE OF CLC CHLORIDE CHANNELS: Structure, Mechanism, and Many Unsettled Questions, <i>Merritt Maduke, Christopher Miller, Joseph A. Mindell</i>	411
DESIGNED SEQUENCE-SPECIFIC MINOR GROOVE LIGANDS, <i>David E. Wemmer</i>	439
PULSED AND PARALLEL-POLARIZATION EPR CHARACTERIZATION OF THE PHOTOSYSTEM II OXYGEN-EVOLVING COMPLEX, <i>R. David Britt, Jeffrey M. Peloquin, Kristy A. Campbell</i>	463

ELECTROSTATIC MECHANISMS OF DNA DEFORMATION, <i>Loren Dean Williams, L. James Maher III</i>	497
STRESS-INDUCED STRUCTURAL TRANSITIONS IN DNA AND PROTEINS, <i>T. R. Strick, J.-F. Allemand, D. Bensimon, V. Croquette</i>	523
MOLECULAR MECHANISMS CONTROLLING ACTIN FILAMENT DYNAMICS IN NONMUSCLE CELLS, <i>Thomas D. Pollard, Laurent Blanchoin, R. Dyche Mullins</i>	545
UNNATURAL LIGANDS FOR ENGINEERED PROTEINS: New Tools for Chemical Genetics, <i>Anthony Bishop, Oleksandr Buzko, Stephanie Heyeck-Dumas, Ilyoung Jung, Brian Kraybill, Yi Liu, Kavita Shah, Scott Ulrich, Laurie Witucki, Feng Yang, Chao Zhang, Kevan M. Shokat</i>	577